SMART DISTRIBUTION TRANSFORMER FOR SMART GRID

A Thesis

by

TAEYONG KANG

Submitted to the Office of Graduate and Professional Studies of
Texas A&M University
in partial fulfillment of the requirements for the degree of

MASTER OF SCIENCE

Chair of Committee,	Prasad Enjeti
Committee Members,	Shankar P. Bhattacharyya
	Mehrdad Ehsani
	Zhizhang Xie
Head of Department,	Miroslav Begovic

May 2016

Major Subject: Electrical Engineering

ABSTRACT

In this thesis, a smart distribution transformer which improves power quality in the electrical power distribution grid is discussed. The proposed system is comprised of an existing line frequency (LF) distribution transformer connected to a power electronic module that is 'auto-connected' on the secondary side. The auto-connection is facilitated by utilizing a high-frequency (HF) / medium frequency (MF) transformer in the power electronics module. A simplified method to compensate for voltage sags and swells on the grid side by providing continuous ac voltage regulation is presented. When a voltage sag and swell event occurs, the power electronic module generates a compensating voltage which is vector-added to the grid voltage in order to supply the regulated output voltage to the load. The smart distribution transformer will satisfy the various needs of the present and future distribution smart grid such as improved availability, equipment protection, and resilience. In this thesis, detailed analysis, simulation and experimental results are discussed to validate the proposed smart distribution transformer.

ACKNOWLEDGEMENTS

The Foremost, I would like to express my gratitude to my advisor, Dr. Prasad Enjeti for his patience, motivation and encouragement. His guidance has been invaluable to this research. I would also like to thank my committee members, Dr. Ehsani, Dr. Bhattacharyya, Dr. Xie for their guidance and support throughout the course of this work. A special thanks to Tammy Carda, and Melissa Sheldon for their support in navigating different aspects of graduate school.

I have greatly benefited from the company of my colleagues at Power Quality Laboratory. I thank my fellow lab mates Harish, Soma, Bahaa, Jorge, Jose, Michael, Dibyendu, Pawan, Ahmed, Yong, Weiran Sinan, Fahad, Salwan, Angela and others for making my time at Texas A&M University a great experience. I would like to express my gratitude to Dr. Sewan Choi for his support during his sabbatical period.

Finally, thanks to my mother, father and brother for their support, patience and love.

TABLE OF CONTENTS

Page

LIST OF FIGURES

Page

LIST OF TABLES

Page

1. INTRODUCTION AND LITERATURE REVIEW

1.1. Introduction

This work presents a new type of distribution transformer as a retro-fit to the conventional distribution transformer without replacing the existing distribution transformer for smart grid. Today, the feature of distribution system has experienced transformational changes by developing of power electronics and renewable distributed generations. The smart grid presents flexible and reliable energy distribution through a bi-directional dialog between the supplier control center and the smart meters on the user-side. As distributed generation and renewable energy system are key technologies in smart grid system, their impact on the power quality issues cannot be underrated.

1.2. Introduction of Distribution Transformer

Therefore, highly reliable and high-quality electricity supply is critical in smart grid. The distribution transformer is a fundamental component in providing high-quality electricity to the end-consumer such as commercial, industrial residential applications as shown in Figure.1.

Distribution transformer is available in the market in various size and efficiencies depending upon the purpose and budget of the end consumers. Secondary terminals of distribution transformer deliver electrical power at a utilization voltage level to the end-user and there are several types of transformer utilized in the distribution system. A typical type of single phase distribution transformer is utilized in United States of America for supplying single phase residential applications [1].

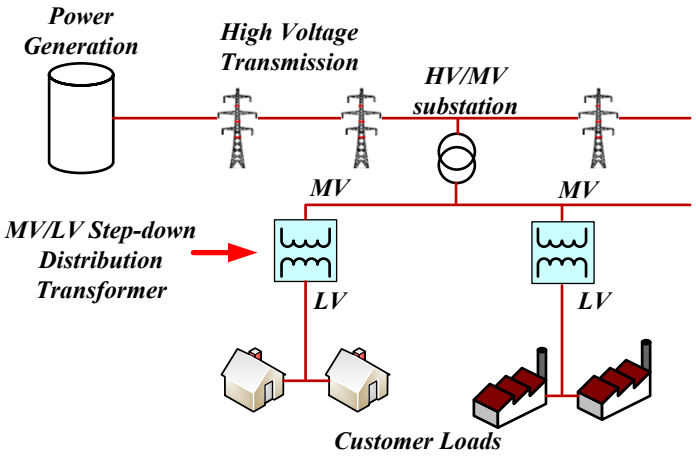

Figure 1. Concept of Functionality of Distribution Transformers in Electric Grid

The residential single phase load is generally required single type pole mounted transformer. This type of pole mounted distribution transformer consisted of total three secondary terminals. Two of them are phase terminals and one of them is ground. Two phase wires delivers 240 volts across them, and the voltage across each phase and ground is 120 volts. Therefore, an end-consumer is able to supplied either 240 volts or 120 volts depending upon the requirement.

1.3. Power Quality Issues in Distribution Grid

Although the conventional distribution transformer is relatively durable and reliable depending upon its requirement, it is not assured to protect loads from nuisances such as poor grid voltage regulation under load, poor performance under voltage disturbances (sag/swells/distortion) and sensitivity to harmonics.

Poor power quality issues have been a more paramount concern of both power supplier and customers. Although there have had much efforts and investments by utility

to prevent power interruptions, it is not possible to completely control disturbances on the supply system. The aging distribution grid infrastructure and the incompatibility between present load features and the electric power supply environment cause occurrence of poor power quality. This results in significant economic losses in a wide range of areas. It is estimated that deteriorated power supplies cost customers around the world millions of dollars [3] as shown Table 1 and Table 2.

TABLE 1. COST OF VOLTAGE OF DISTURBANCE (INDUSTRY) / FINANCIAL LOSS

(© 2012 IEEE) [3]

Industry/sectors	**Typical Financial loss per event (USD)**
Semiconductor production	5579
Financial trading	8820/hour
Data center	1103
Telecommunications	45/min
Steel works	515
Glass manufacture	368
Offshore platforms	375-1100/day
Dredging / Reclamation	75-400/day

TABLE 2 COST OF VOLTAGE DIPS (COUNTRY) (© 2012 IEEE) [3]

Cost of Voltage Dips (Sags)		
Industry	Duration	Cost/Sag
U.K. steeworks	30% for 3.5 cycles	$457447
US glass plant	Less than 1s	$200
US petrochemicals	2s	$600
US	Annual Exposure	$10M
South Africa	Annual exposure	$3B

1.4. Voltage Sag and Swell

Voltage sag is a reduction in voltage compared to normal rated voltage and voltage swell is an increase in voltage outside normal rated tolerance of loads as shown in Figure.2. The voltage sag and swell are the most critical power quality issues in distribution grid today [2]. The survey of power quality presents that voltage sags with 40-50% of the nominal value and with duration from 2 to 30 periods occurred in about 92% of all power system events [4-7].

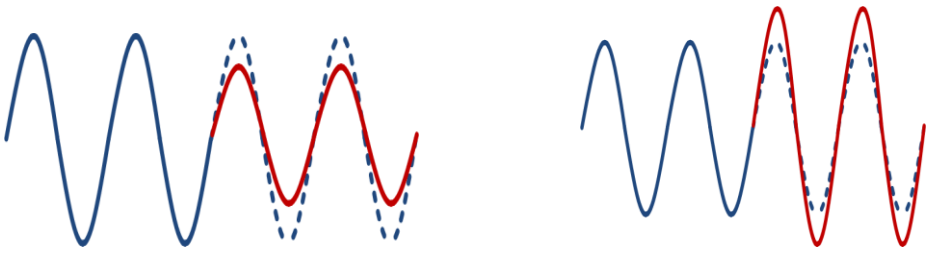

(a) (b)

Figure 2. (a) Voltage Sag (Left) (b) Voltage Swell (Right).

The acceptable over and under-voltage ranges for grid power supply is introduced in Figure.3 and Figure.4 [4]. Figure.3 shows the Computer Business Equipment Manufacturing Association (CBEMA) power acceptability curve which indicates rated voltage with logarithmic scale in seconds. The CBEMA curve has an upper limb locus that represents the boundary of acceptable/unacceptable operation for over voltages and under voltages. Also, there are other similar curves contains a power acceptability which is the Information Technology Industry Council (ITIC) curve shown in Figure.4.

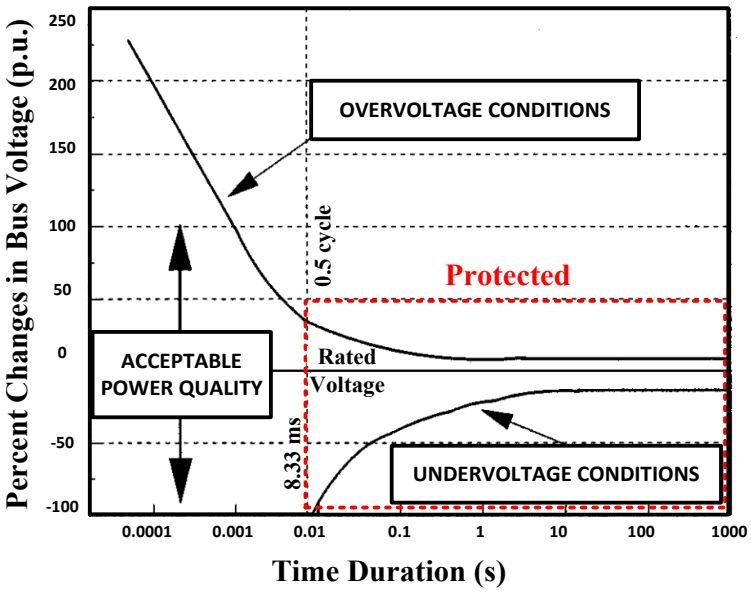

Figure 3. *CBEMA* Power Acceptability Curve (© 2002 IEEE) [4].

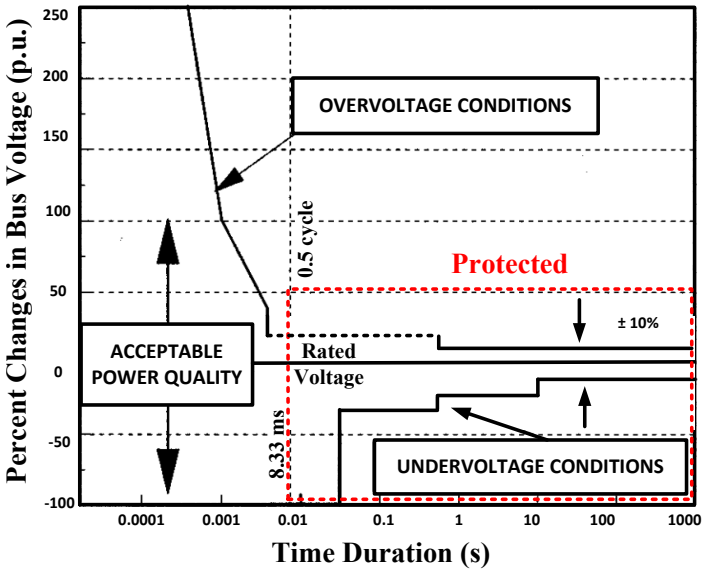

Figure 4. *ITIC* Power Acceptability Curve (© 2002 IEEE) [4].

According to CBEMA and ITIC power acceptability as shown in Figure 3 and 4, it is suggested to consider new type of distribution transformer function for a wider range of voltage compensation over a long dynamic period.

1.5. Literature Review

1.5.1. On-load tap changers

The most common voltage compensator for distribution transformer is the automatic on-load tap changers, which are fitted to most distribution transformers throughout the systems. However, poor dynamic of ac voltage compensation, stepwise variation and a narrow range of output regulation are major issues to solve in order to achieve a rapid response to voltage disturbance [8-10]. Furthermore, the tap changers can be often

utilized in no-load condition so that it is required to make a disconnection the load in order to obtain variable output voltage.

1.5.2. Pulse-width modulation ac/ac converter

Another approach to mitigate voltage disturbances is based on power electronics, which guarantee good dynamic characteristics by utilizing ac-ac Pulse-width modulation (PWM) converter [5-7]. Dynamic sag correctors (DySC) and ride-through voltage compensators can resolve power quality problems on a customer's distribution line by providing voltage dip mitigation at reduced cost [5] as shown in Figure.5. In other works, a PWM ac-ac buck converter with auto-transformer to process partial load-power was discussed to compensate for voltage sags [7]. However, systems introduced in [5-7] has a limitation that it is possible to compensate only for voltage sags.

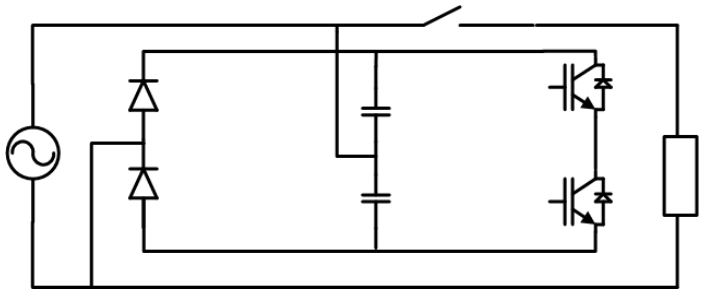

Figure 5. Dynamic Sag Correctors (Dysc) [5].

1.5.3. Dynamic voltage restorer (DVR)

Additionally, an often encountered approach for sag/swell mitigation is the dynamic voltage restorer (DVR) injecting a voltage component in series with the load voltage

[11-13]. The DVR with its dynamic capabilities is able to compensate for voltage sag/swell restoring line voltage to its nominal value and hence avoiding any power disruption to the load. Also, a voltage sag/swell compensator using direct power conversion was proposed without dc-link capacitors [14]. However, these compensators have some limitations such as the requirement of a bulky line frequency transformer and/or huge energy storage capacitors causing challenges in integrating them with existing line-frequency distribution transformers.

1.5.4. Hybrid distribution transformer

A new concept called the hybrid distribution transformer was introduced to regulate output voltage by utilizing a partial power electronic module [15-17]. This approach can provide dynamic voltage regulation under both voltage sags and swells for non-linear load conditions with galvanic isolation as shown in Figure.6. The addition of a power electronic module provides the passive distribution grid components a controllable functionality for the utility. With the increased controllability of the distribution grid enables to achieve higher quality of electricity for the end-customer.

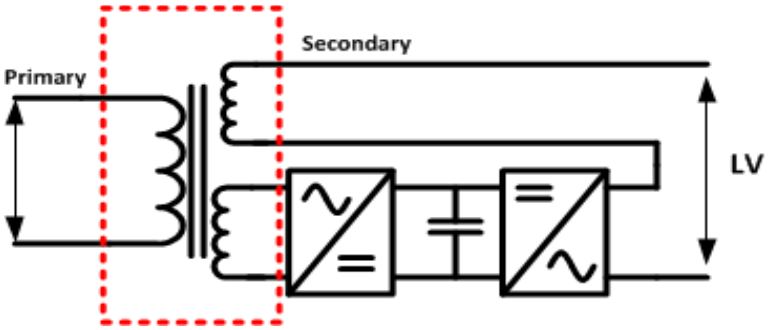

Figure 6. Hybrid Distribution Transformer Schematic [15].

However, this approach requires additional windings on the existing bulky line-frequency transformer, thus increasing the size and weight of transformer with greater replacement cost [18].

1.6. Research Objective

As discussed in the precious section, the various methods for voltage disturbance compensation have been studied rigorously in the literature. Through a number of different approaches exist which address these problems separately, none of the discussed methods which is able to be covered all requirements as a single solution. The objective of this research is to develop a retro-fit solution for the conventional distribution transformer in order to improve power quality in distribution system.

Recently, the power electronic transformer (PET) has been extensively investigated for use in distribution systems, functionally replacing the traditional transformer. Reducing the size of PET by using a either a Medium Frequency (*MF*) or a High Frequency (*HF*) transformer with power electronic devices provides an improved efficiency compared to that of a conventional transformer with the same ratings [19-20].

In the thesis, the proposed transformer is realized by employing a MF/HF transformer with fractional rating power ctronics along with auto-transformer configuration (Figure. 7).

Figure 7. Concept of Smart Distribution Transformer Scheme Including Power Electronics Module for Smart Grid.

The specific requirements for smart distribution transformer over existing distribution transformers are same as followings:

- The proposed topology is required to be an easy retro-fit solution, without modifying existing distribution transformers; hence high power density is necessary.
- A wider range of voltage disturbances compensation is required with fast dynamic capabilities to its nominal values.
- Under external fault conditions, the bypass switch SW can protect the PE module from over current.
- No line frequency transformer or bulky energy storage capacitors such as electrolytic capacitors are required in the power electronic module, resulting in reduced size and weight.

- Fractionally rated power electronics module is required to make the overall system one with lower cost and higher reliability.

1.7. Conclusion

The distribution transformer is fundamental component for distribution system and widely utilized in continuous process smart grid. Any disturbance of electricity has significant financial impact, hence the power quality issues cannot be neglected to deliver high quality electricity to end-consumer. A variety of types for voltage disturbance compensation are reviewed and summarized. A detailed discussion on the existing solutions and their limitations were presented. The research objective and thesis organization were introduced in the end.

2. CONCEPT AND TOPOLOGY OF SMART DISTRIBUTION TRANSFORMER*

2.1. Introduction

This chapter presents a concept and characteristics of the proposed system. The fundamental operation of compensating voltage sag/swell is covered in terms of mathematical approaches in this chapter. Moreover, switching operation and partial rated power process of the proposed system are explained.

2.2. Concept of Smart Distribution Transformer

A conceptual schematic of the smart distribution transformer is as shown in Figure.8. The proposed smart distribution transformer is composed of two parts – a line frequency (50/60Hz) pole top distribution transformer and a power electronic (*PE*) module. The existing line distribution transformer is able to be retrofitted with *PE* module; hence it is not required to replace the existing distribution transformer, as shown in Figure.8. This requires no extra winding on the bulky line frequency transformer, hence reducing the size and weight of distribution transformer with greater replacement cost for the voltage compensation capability.

---

* *Reprinted, with permission, from Kang, T.; Essakiappan, S.; Enjeti, P.; Choi, S.; "Towards a smart distribution transformer for smart grid", 9th International Conference on Power Electronics and ECCE Asia(ICPE-ECCE Asia) 2015, Seoul, South Korea, pp. 1997-2003 © 2015 IEEE.*

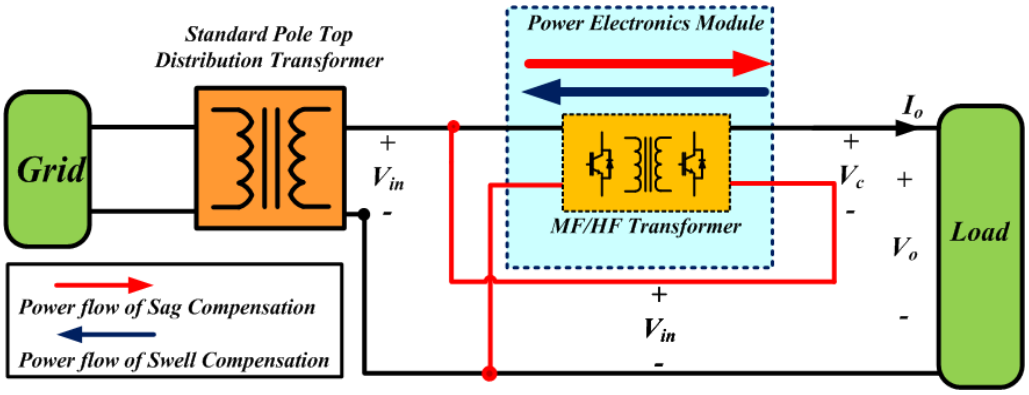

Figure 8. Conceptual Scheme of the Proposed Smart Distribution Transformer with Power Electronics Module.

One secondary side terminal of the line frequency transformer is connected to an output terminal of the *PE* module so that the load voltage is the sum of the compensating voltage of the *PE* module (V_c) and the secondary side voltage of the standard distribution transformer (V_{in}). Consequently, it is possible to compensate voltage in the load side without any energy storage components due to auto-connection between line frequency transformer and power electronics module. Furthermore, only partial power is processed through the *PE* module during the system operation, which results in a decreased power rating of the *P*E module.

During a voltage sag, (i.e.,$|V_o| > |V_{in}|$), a compensating voltage, V_c from the *P*E module adds to the source voltage (V_{in}), as shown in Figure.9(a).

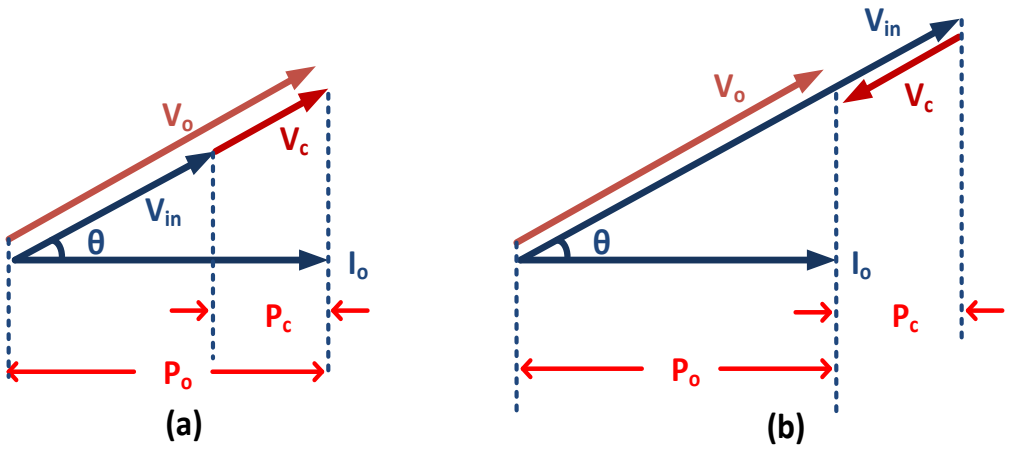

Figure 9.Voltage Vectors for the Compensation of (a) A Voltage Sag and (b) a Voltage Swell.

If a voltage swell occurs, (i.e.,$|V_o| < |V_{in}|$), the *PE* module produces a 180° out-of-phase compensating voltage, as shown in Figure.9(b). The power flow of the compensating power is reversed compared to that of the load during the swell condition. The compensating voltage (V_c) is generated from power electronics module and this V_c is added to the load voltage depending on sag or swell condition by auto-connection method between line-frequency transformer and power electronics module. The compensated active power (P_c) from *PE* module is defined as

$$P_c = \left[|V_o| \cdot \cos\theta - |V_{in}| \cdot \cos\theta\right] \cdot |I_o| = |V_c| \cdot \cos\theta \cdot |I_o| \quad (1)$$

where θ is the load power factor angle. Since the phase of the adding compensating voltage V_c is 180° delayed in swell condition, the precise voltage sag and swell detection algorithms are required to achieve in this approach. The detailed voltage disturbance detection algorithm and control system will be covered in chapter 3.

2.3. Architecture of the Power Electronics Module in Smart Distribution Transformer

The detailed schematic diagram of the *PE* module for the smart distribution transformer is shown in Figure.10. The *PE* module consists of four single-phase H-Bridge converters, *MF*/*HF* transformer, output filter, static bypass switches and DSP controller as seen in Figure.10. Two H-bridge converters (M_2, M_3) connected directly to the *MF*/*HF* transformer operate at a high switching frequency while the other two converters (M_1, M_4) operate at line frequency. Each H-bridge converter has four insulated-gate bipolar transistors (*IGBT*) for fast switching in order to operate single phase converter and inverter.

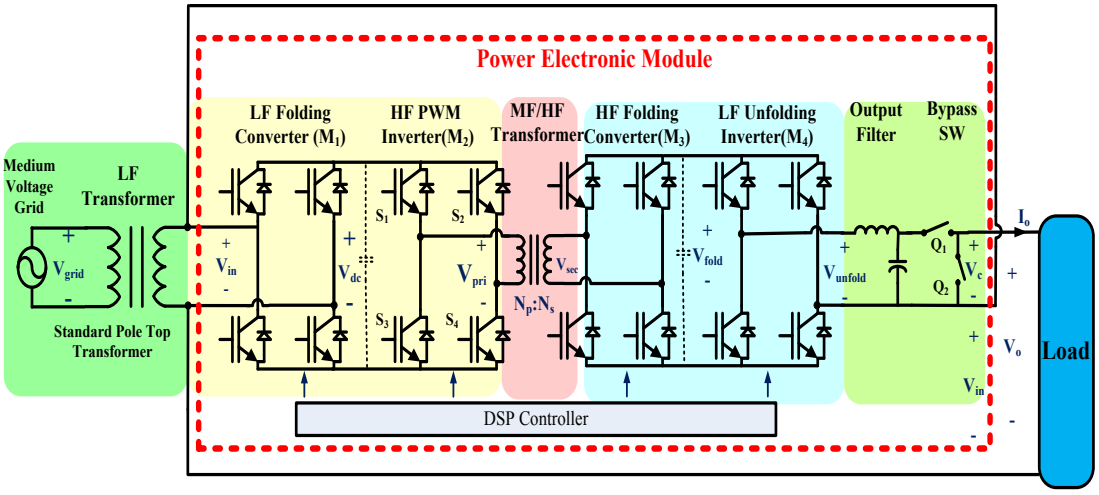

Figure 10. Detailed Power Electronics Module in the Proposed Smart Distribution.

The PE module operates in voltage compensation mode or bypass mode. During bypass mode, the grid-side voltage (V_{in}) is directly connected to the load-side by closing

a bypass switch Q_2. When voltage disturbances (sag / swell) occur on the grid-side, the bypass switch Q_2 is opened and Q_1 is closed so that the PWM switches are activated to supply the required compensating voltage (V_c).

The *MF*/*HF* transformer is the key of the proposed structure. The size/weight reduction of the transformer in the PE module is achieved by .*MF/HF* operation. Since the smart distribution transformer is retro-fit solution as discussed in previous chapter 1, it is critical to reduce the size of power electronics module. Thus, high power density is able to be achieved by utilizing *MF/HF* transformer in the power electronics module. The *MF/HF* transformer core can be designed with conventional silicon steel and the operating frequency can be selected from 1kHz to higher than 20kHz. A *HF* transformer can be employed for relatively higher power applications, while a *HF* transformer may be preferred for lower power residential-type applications [20] [21].

2.4. Operating Principal of the Power Electronics Module

The front-end of the PE module, M_1 is a single-phase rectifier hereby addressed a 'Low frequency (*LF*) folding converter. Figure.11(a) shows the input of power electronics module which is needed to be compensated in voltage disturbance occurrence condition. The *LF* folding converter operates at line frequency (50 / 60Hz) (see Figure.11 (b)) as a synchronous rectifier. It is generated pulsating dc from the ac source as shown in Figure.11(c) since there is no bulky energy storage component such as dc-link capacitor. The pulsating double frequency voltage ripple can be expressed as

$$V_{dc} = \sqrt{2} \cdot V_{rms} \left(\frac{2}{\pi} - \frac{4}{\pi} \sum_{n=2,4,6\ldots}^{\infty} \frac{\cos(n\omega_o t)}{n^2 - 1} \right) \tag{2}$$

A *MF/HF* voltage is generated from the pulsating dc voltage by the *HF PWM* inverter (*M_2)* using the proposed phase-shifted modulation technique. The phase shift angle, ϕ is adjusted in order to regulate load voltage as shown in Figure.11 (d). The switching function S_{M2} for the converter M_2 is shown in Figure.11 (e) and can be described as

$$S_{M2} = \frac{4}{\pi} \cdot \sum_{n=1,3,5\ldots}^{\infty} \frac{1}{n} \cdot \sin\left(n\omega_s t + \frac{\pi - n\phi}{2}\right) \cdot \sin\left(\frac{n\phi}{2}\right) \tag{3}$$

Therefore, the primary voltage of the *MF/HF* transformer is shown in Figure.11(f) and is given as

$$V_{primary} = \left(1.62 \cdot \sqrt{2} \cdot V_{rms}\right) \cdot \begin{bmatrix} \sin(\omega_s t + \frac{\pi-\phi}{2}) \cdot \sin(\frac{\phi}{2}) - \frac{1}{3}\sin(3\omega_s t + \frac{\pi-3\phi}{2}) \cdot \sin(\frac{3\phi}{2}) \\ + \frac{1}{3\pi}\sin\left\{(\omega_s \pm 2\omega_o)t + \frac{\pi-\phi}{2}\right\} \cdot \sin(\frac{\phi}{2}) - \frac{1}{3\pi \cdot (3)} \cdot \sin\left\{(3\omega_s \pm 2\omega_o)t + \frac{\pi-3\phi}{2}\right\} \cdot \sin(\frac{3\phi}{2}) \\ \cdots \\ + higher\ order\ terms \end{bmatrix} \tag{4}$$

Note that V_{pri} has no low frequency components such as line frequency or its harmonic components, and the major frequency component of the *MF/HF* transformer are odd multiples of the switching frequency ω_s and their sideband components $\omega_s \pm 2\omega_o$, as seen in (4). Since there is no line frequency components in Fourier series expression of primary voltage V_{pri}, but only higher frequency components, *MF/HF* transformer can be connected directly *HF PWM* inverter (*M_2)* in the power electronics module; hence, higher power density can be achieved in this structure.

If the switching function S_{M2} for the converter M_2 has positive or negative values, power is delivered to power electronics module. Otherwise there is no power can be delivered when switching function is zero value. During normal condition mode that there is no voltage disturbance in grid side, the phase angle, ϕ would be zero degree between left leg and right leg bridges in the converter M_2 generating the zero compensating voltage at the output side of power electronics module. In other words, the bypass mode of the power electronics module is activated when the phase angle ϕ meet the zero degree which is supplied normal voltage from the grid. For this reason, the phase angle, ϕ in primary voltage, V_{pri} is determined by the amount of compensating voltage which is required to supply nominal voltage in load side. Therefore, the compensating voltage which will be added to the load voltage can be dynamically generated by adjusting the phase angle ϕ of the converter M_2. The derivation of the phase angle, ϕ will be discussed in control strategy section in chapter 3.

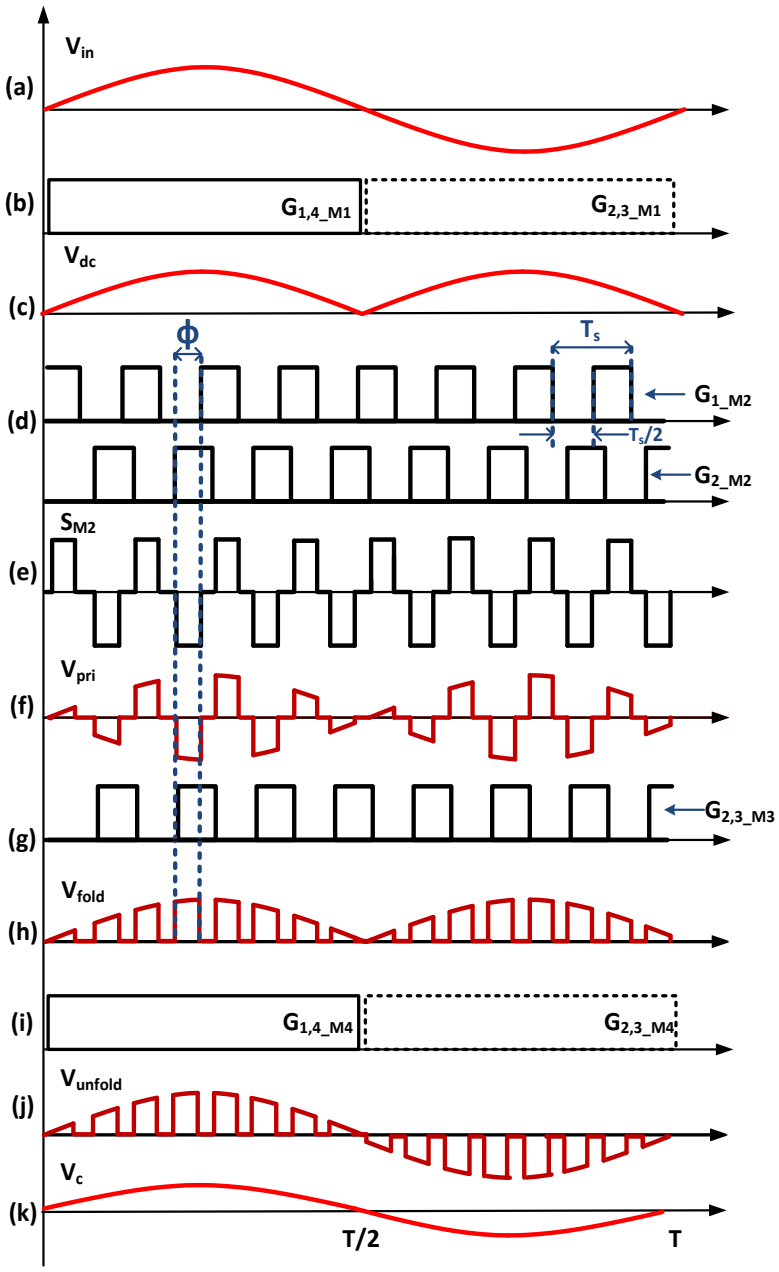

Figure 11. Ideal Operating Waveforms of PE Module for Sag Operation (a) Source Voltage, V_{in}. (b) M_1 Gate Signal, G_{M1}. (c) LF Rectified Voltage, V_{dc}. (d) M_2 Gate Signal, G_{M2}. (e) Switching Function of M_2, S_{M2}. (f) Primary Voltage of MF/HF Transfomrer, V_{pri}. (g) M_3 *Gate Signal*, G_{M3}. (h) LF Folded Voltage, V_{fold}. (i) M_1 Gate Signal, G_{M1}. (j) LF Unfolded Voltage, V_{unfold}. (k) Compensating Voltage, V_c.

The secondary side of the *MF/HF* transformer also has similar *HF* folding converter, M_3 followed by the *LF* unfolding inverter as shown in Figure.10. The M_3 converter operates as a *HF* synchronous rectifier and generates the *HF* voltage of the secondary side, which is a double frequency voltage as seen in Figure.11(h). In the *LF* unfolding converter M_4, the gate signal operates at the line frequency (50/60Hz) as seen in Figure.11(i). The function of the *LF* unfolding converter M_4 is to unfold *HF* rectified voltage in line frequency (50/60Hz) in order to generate ac voltage by filtering out *HF* components. In case of the sag, diagonal switches $S_{1,4\_M4}$ are closed during positive half cycle of *LF* sinusoidal voltage signal as shown in Figure.11(j). During a swell condition, the output voltage of M_4 generates a 180° out-of-phase compensating voltage. Afterward, a small output filter attenuates the *HF* components in the compensating voltage, V_c (seen in Figure.11(g)).

2.5. MF/HF Transformer Turns Ratio of Power Electronics Module

The compensating voltage, V_c is regulated to be the difference between grid-side voltage V_{in} and the desired load voltage ($V_{o,ref}$), as seen in (5).

$$V_c = V_{o,ref} - V_{in} \tag{5}$$

Set the required compensating voltage, V_c to be

$$V_c = -k \cdot V_{o,ref} \tag{6}$$

where "k" represents the amount of voltage sag/swell magnitude per unit ($k < 0$ for sag and $k > 0$ for swell), e.g. V_c = -0.2V_o for a 20% voltage swell case, and $V_c = 0.3V_c$ for *a* 30% voltage sag case.

Then, the grid-side voltage V_{in} can be expressed from (5) and (6) by

$$V_{in} = (1+k) \cdot V_{o,ref} \tag{7}$$

From Figure.9, the output of PE module V_c, the required compensating voltage, is described as

$$V_c = V_{in} \cdot \frac{\phi}{\pi} \cdot \frac{N_p}{N_s} \tag{8}$$

where $\phi \in [0,\ \pi]$

Hence, the compensated load side voltage, $V_{o,ref}$ can be expressed as

$$V_{o,ref} = (1+k) \cdot V_{o,ref} + \frac{\phi}{\pi} \cdot (1+k) \cdot V_{o,ref} \cdot \frac{N_p}{N_s} \tag{9}$$

Consequently, the relationship between the *MF/HF* transformer turns ratio N_p:N_s and the range of the compensation voltage sag/swell becomes

$$\frac{N_p}{N_s} = \frac{\pi}{\phi} \cdot \left| \frac{k}{1+k} \right| \tag{10}$$

From (10) the range of the compensation for the sag/swell relative to the phase angle ϕ can be obtained as shown in Figure.12. It is seen that voltage sags up to 50% of grid voltage could be compensated when N_p:N_s ratio is 1:1. The variation of the phase shift angle ϕ for the sag compensation is wider than that of the swell compensation as seen in Figure.12.

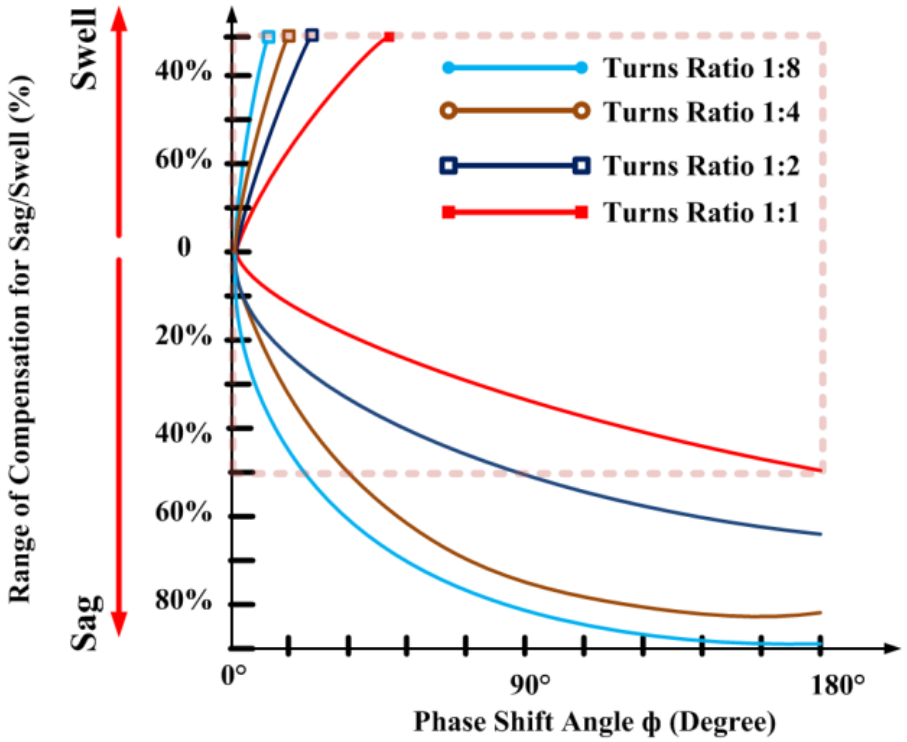

Figure 12. Phase Shifting Angle Variation as Turns Ratios Changes in the PE Module.

It is noted that the phase shift angle ϕ can be determined by the amount of voltage sag/swell that is required to be compensated. Based on equation (10), turns ratio of the MF/HF transformer depends on the phase shift angle, ϕ and the amount of voltage sag/swell magnitude per unit, k. Therefore, the wider range of voltage disturbance can be achieved by increasing turns ratio of MF/HF transformer as shown in Figure.12.

2.6. Switching Operation in Phase-Shift Modulation

The PWM inverter and folding converter are required actively control the bidirectional power flow while regulating load voltage. In this system, the phase-shift modulation is implemented as discussed in II.3. The control method regulates power

flow through adjusting the phase delay between the gate signals of diagonal IGBTs in the bridge which are Q1 and Q4 in Figure.13.

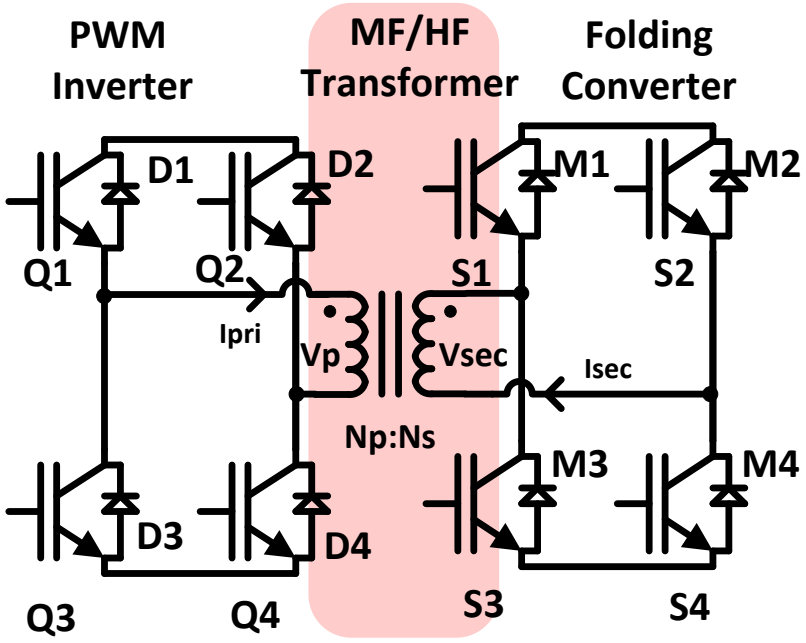

Figure 13. Schematic of HF PWM Inverter and HF Folding Converter.

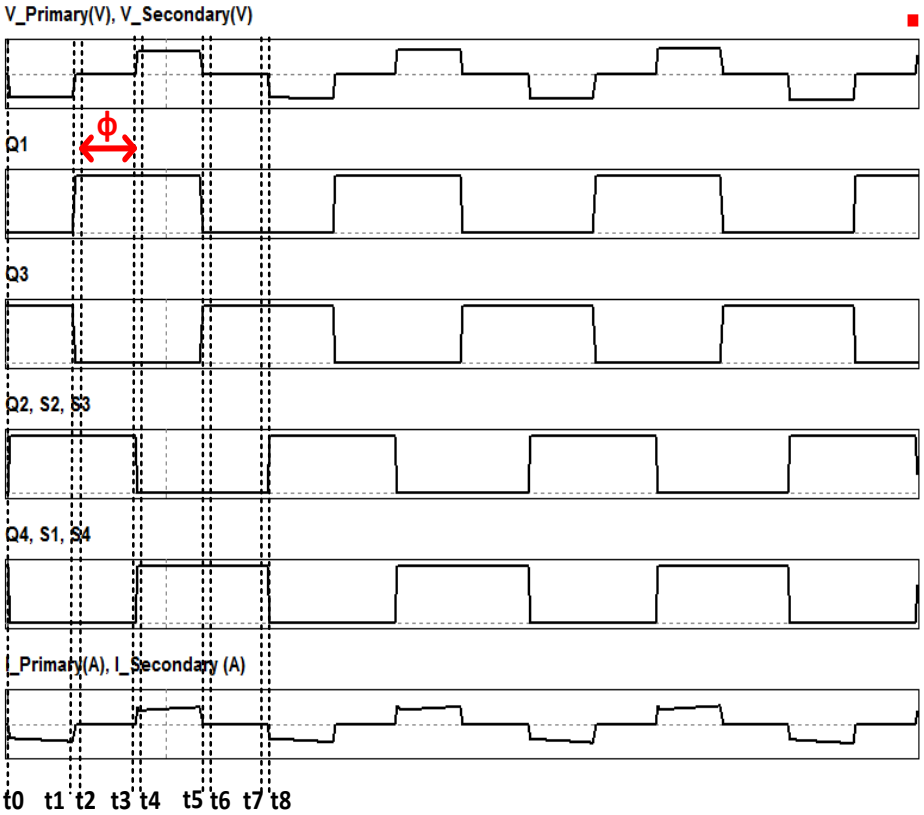

Figure 14. Waveforms and Switching Functions in Phase-Shift Modulation Control.

Figure.14 shows the ideal waveforms of the phase-shift modulation in operation from source to load which is in the sag case. The 50% duty-cycle gate driving signals of Q2 is shifted ahead of Q1 by phase-shift angle ϕ which is positive. The gate signals of S1, S4 and Q4 are synchronous, and the gate signals of Q2, Q3, S2, and S3 are complementary 50% duty cycle signals.

The conducting switches are shown in Table.3. The secondary side switches perform as synchronous rectifiers during power flow from source to load side. In this case, passive switches of secondary side are utilized to deliver power. Also, the magnetizing

current is passed through active switches in secondary side of transformer during zero voltage state. During the dead time, current I_p freewheels through one of active switches and one of diodes in the primary transformer side.

TABLE 3 TABLE OF CONDUCTING SWITCHES IN PHASE SHIFT MODULATION

Period	**Conducting Switches**	
	Primary Side	**Secondary Side**
t0-t1 (Vpri : -V)	Q2, Q3 ON	M2, M3 Conduct
t1-t2 (Dead Time)	Q2, D1 Conduct Freewheeling state	S2, S3 ON
t2-t3 (Vpri : 0V)	Q1, Q2 ON	S2, S3 ON
t3-t4 (Dead Time)	Q1, D2 Conduct Freewheeling state	M4, M1 Conduct
t4-t5 (Vpri : +V)	Q1, Q4 ON	M1, M4 Conduct
t5-t6 (Dead Time)	Q4, D3 Conduct Freewheeling state	S1, S4 ON
t6-t7 (Vpri : 0V)	Q3, Q4 ON	S1, S4 ON
t7-t8 (Dead Time)	Q3, D4 Conduct Freewheeling state	M2, M3 Conduct

2.7. Comparison of Range for Voltage Sag/ Swell Compensation

In this section, the comparison of range for compensation range in the proposed system compared to previous approaches is discussed. In the chapter 1, a variety of types for voltage disturbance compensation are reviewed. Figure.15. shows a comparison of the range for voltage compensation for four different types of distribution transformer – electromagnetic tap changer, dynamic sag corrector, hybrid distribution transformer and the proposed distribution transformer [5-17]. First, electromagnetic tap changer has relatively narrow range for voltage disturbance compensation [8-9] and dynamic sag corrector has only capability for sag compensation up to 50% sag condition [5].In case of hybrid distribution transformer, voltage sag and swell compensation can be covered by 50% respectively[15]. However, as discussed in previous chapter, a wider range of compensation is required in CBEMA and ITIC power acceptability.

In the proposed system, it is noted that a wide range of compensation can be achieved by optimizing the turns ratio of *MF/HF* transformer in the proposed system as discussed in previous section. Figure.15. shows that 50% voltage sag can be compensated when the turns ratio of *MF/HF* transformer (N_p/N_s) is 1:1. As seen from Figure.15, the number of turns in the *MF/HF* transformer secondary increases it becomes possible to compensate for deeper sag and swell events, e.g. 1:8 turns ratio provides compensation for sag occurrences up to 90%.

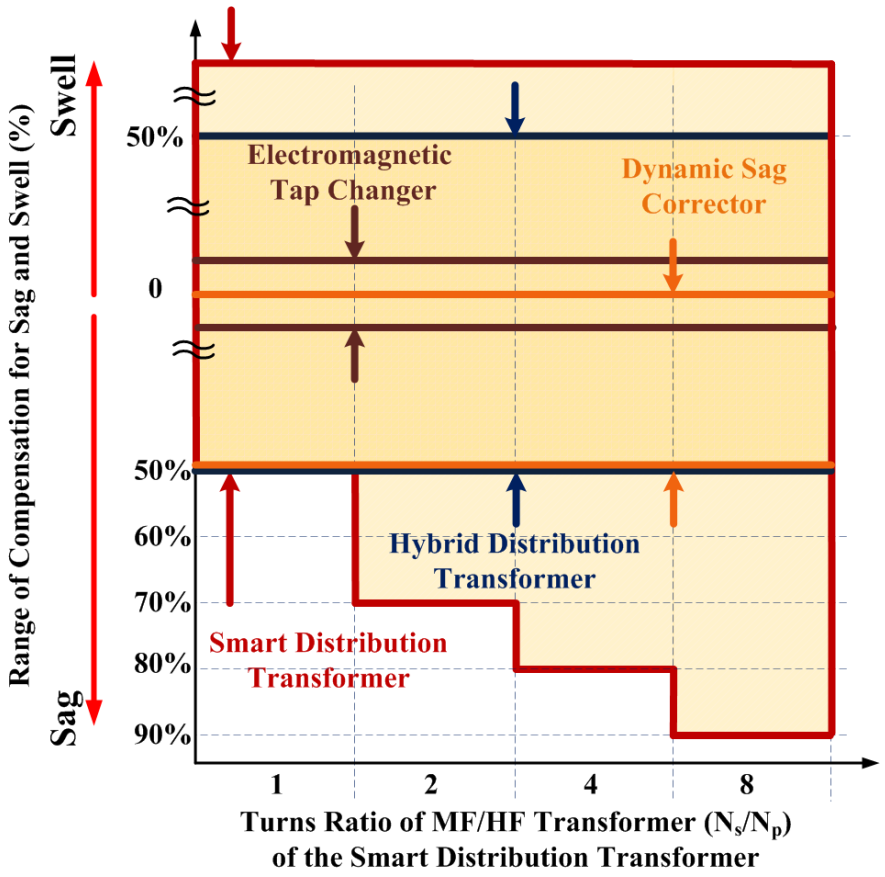

Figure 15. Comparison for Range of Compensation for Voltage Sag/Swell.

2.8. Partial Power Processing of Power Electronics Module

The *VA* ratio of *PE* module to load can be obtained in ideal operations as seen in Tables 4 and 5 as a simulation results in Matlab. Various voltage disturbance conditions are studied from 10% to 50% sag and swell respectively with 1:1 *MF*/*HF* transformer in *PE* module. As seen in Tables 4 and 5, *VA* of primary side of *MF/HF* transformer, *VA* of *PE* module, depends on the voltage required to be compensated.

TABLE 4. VA RATIO POWER ELECTRONICS MODULE TO LOAD FOR SAG CONDITION

Rate (%)	Actual input(V)	V_{out} (V)	I_{out} (A)	VA_{out} (VA)	V_c (V)	I_c (A)	VA_c (VA)	VA_c/VA_{out} (P.U)
50	84.8	119.8	2.40	287.5	59.9	2.4	143.8	**0.495**
40	101.8	119.8	2.40	287.5	47.9	2.4	115.0	**0.397**
30	118.8	119.8	2.40	287.5	35.0	2.4	84.0	**0.296**
20	135.7	119.8	2.40	287.5	23.9	2.4	57.4	**0.181**
10	152.7	119.8	2.40	287.5	12.0	2.4	28.8	**0.093**

TABLE 5. VA RATIO POWER ELECTRONICS MODULE TO LOAD FOR SWELL CONDITION

Rate (%)	Actual input(V)	V_{out} (V)	I_{out} (A)	VA_{out} (VA)	V_c (V)	I_c (A)	VA_c (VA)	VA_c/VA_{out} (P.U)
50	254.5	119.8	2.40	287.5	59.9	2.4	143.8	**0.495**
40	237.6	119.8	2.40	287.5	47.9	2.4	115.0	**0.397**
30	220.6	119.8	2.40	287.5	35.0	2.4	84.0	**0.296**
20	203.6	119.8	2.40	287.5	23.9	2.4	57.4	**0.181**
10	186.6	119.8	2.40	287.5	12.0	2.4	28.8	**0.093**

Based on Tables 4 and 5, the ratio of *MF/HF* transformer *VA* to load *VA* is shown in Figure.16. The *VA* ratio increases as amount of sag or swell increases. In other words, only partial power is processed in the *MF/HF* transformer to compensate for that amount of the voltage sag or swell. Therefore, *VA* rating of *MF/HF* transformer, which is also the *VA* rating of the PE module, can be determined based on the amount of magnitude of voltage disturbance.

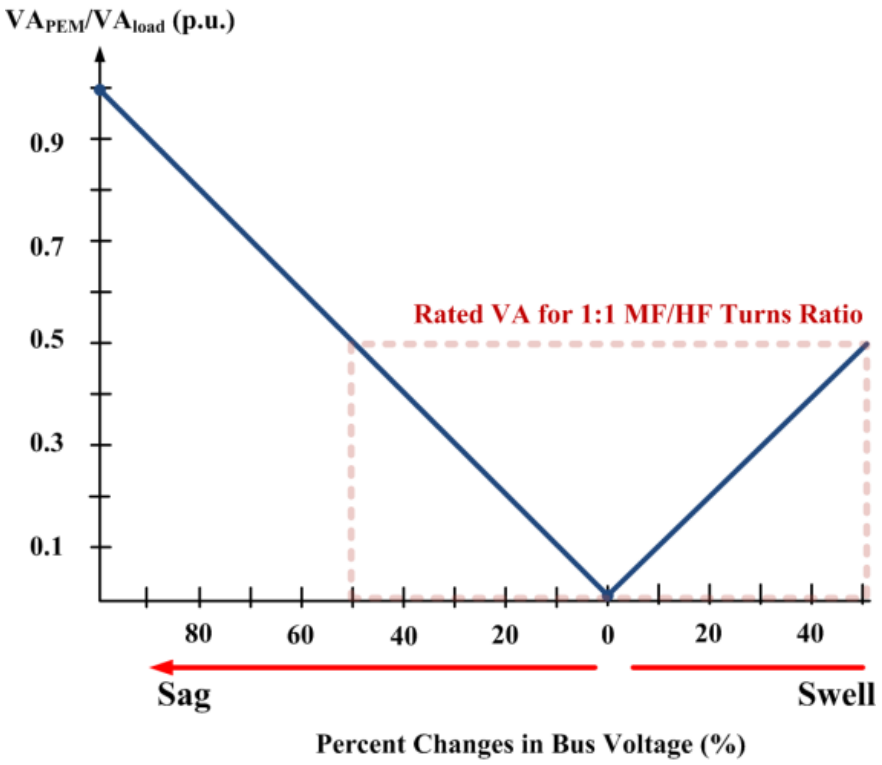

Figure 16. VA Ratio Power Electronics Module to Load.

As shown in Figure.16, only 0.5 per unit partial rated power is required to operate as a 50% sag / swell compensator in the power electronics module with 1:1 *MF/HF* transformer. Hence, the fractional rating of power electronics module can results in lower cost for components depending on the amount of the voltage sag or swell. Also, power electronics module operates only during the voltage disturbance occurred, PE module is not required to have full power casing higher reliability of the system.

Furthermore, the summarized features of the proposed system compared to other approaches discussed in previous section are shown in Table 6, according to the previous literatures.

TABLE 6: SUMMARY OF FEATURES FOR VOLTAGE COMPENSATORS IN GRID DISTRIBUTION

Type	Galvanic Isolation	Voltage Compensation Range	Retrofit Solution to LFT	Usage of Electrolytic Capacitor	Availability of Bypass mode
On-Load Tap Changer [8-10]	Yes	Limited Sag / Swell (Poor dynamic step response)	Yes	No	No
DySC or conventional ride-through system [5-7]	Yes/No (Need extra LFT)	Mostly Sag only	Yes/No	Yes/No (Need energy storage system)	Yes/No
Hybrid Distribution Transformer [15-17]	Yes	Sag / Swell	No (Replacement of whole existing LFT)	Yes	Yes/No
The Proposed System	Yes	Wider Sag / Swell	Yes (Easy Integration)	No (Increase reliability and power density)	Yes

2.9. Conclusion

The proposed smart distribution transformer which is a retro-fit solution to improve power quality is described in this chapter. The *PE* module is attached to existing line frequency transformer; hence it is not required to replace the existing distribution transformer. The proposed distribution transformer has several features over existing distribution transformers:

- Power density of *PE* module can be higher by utilizing Mf/HF transformer.
- No line frequency transformer or bulky energy storage capacitors such as electrolytic capacitors are required in the power electronic module, resulting in reduced size and weight.

- Compensation for wider range of voltage disturbances such as sags/swells is achieved.
- Under normal operating conditions, the power electronics module operates in bypass mode, processing no power; it processes power only during disturbance events, resulting in higher reliability and efficiency.
- Under external fault conditions, the bypass switch SW protects the PE module from over current.
- Fast dynamic capabilities which is able to compensate for voltage disturbance restoring line voltage to its nominal value.
- Fractionally rated power electronics module is required to make the overall system one with lower cost and higher reliability.

3. CONTROL STRATEGY

3.1. Introduction

This chapter presents an operation of the control strategy in the proposed system. The proposed control strategy generates the phase shift angle as an output in order to regulate compensating voltage in the power electronics module. The detailed processes of generating phase shift angle and the voltage detection algorism are explained in this chapter.

3.2. The Proposed Closed Loop Control Strategy

Figure.17 shows the detailed control strategy adopted for the proposed system. It mainly consists of two loops – (a) Load voltage control block with feedback control and (b) Compensating voltage reference generation block with feedforward control. The feedforward loop helps to achieve fast dynamic voltage compensation and is able to respond rapidly to source and load variations. The objective of the feedback control is to reduce the steady-state error in the load voltage. The controller parameters are tuned in order to minimize steady state error and improve the dynamic performance. When the source voltage sag/swell occurs, the compensating voltage reference generation block generates duty ratio, D_{ff} based on the amount of compensating voltage. Also, the load voltage control block generates duty ratio, D_{fb} to regulate the desired load voltage. In the proposed control scheme, the output is phase shift angle, ϕ and this is utilized to determine the amount of compensating voltage as discussed in previous section.

Moreover, as shown in Figure.17, it is noted that gate signals of each *M1*, *M2*, *M3*, and *M4* converters in the PE module are generated by implementing zero crossing angle θ_{PLL}, phase shift angle ϕ and normalized source voltage signal $V_{c,ref}$.

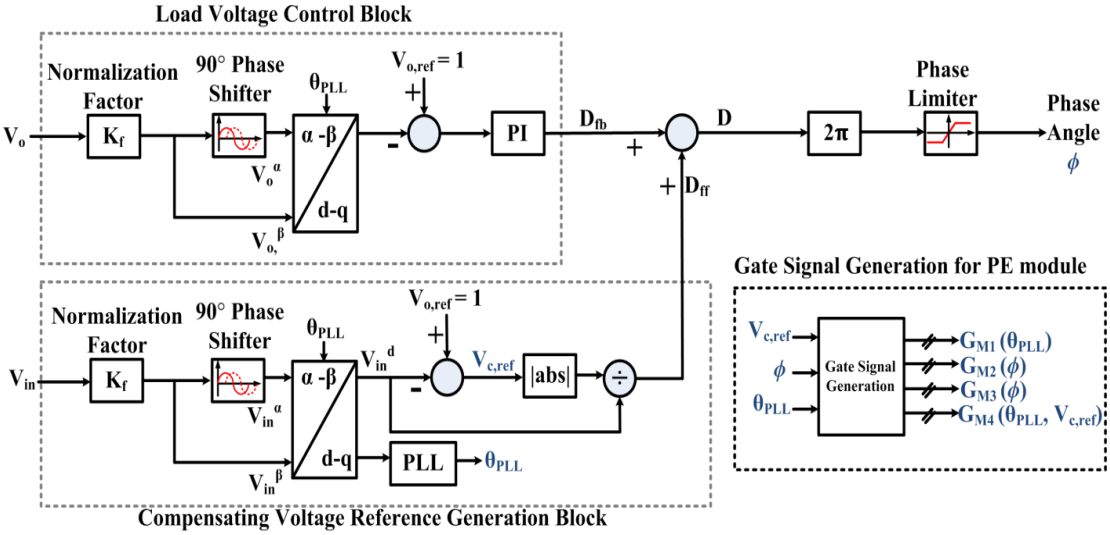

Figure 17. Control Scheme for the Proposed PE Module.

3.3. Voltage Sag and Swell Detection

In order to detect precise voltage sag and swell, a single-phase phase-locked-loop (*PLL*) is utilized. The *PLL* provides the reference phase angle for modulation signal generation. A single-phase alpha-beta / direct-quadrature (*αβ-dq*) transformation generates the direct component which gives the phase angle as well as the peak of the system input voltage. The orthogonal signal necessary for this transformation is generated by means of all pass filters, which introduce a 90° phase shift.

As shown in Figure.17, sensed values of the normalized load and source voltage, multiplied by normalization factor, are utilized to generate the 'd' and 'q' components. By synchronizing the *PLL* rotating reference frame and the utility voltage vector, quadrature axis reference voltage (V_{in}^{q}) and direct axis voltage signal (V_{in}^{d}) can be obtained. In the compensating voltage reference generation block, direct axis component of the input voltage, V_{in}^{d} is obtained and is expressed as

$$V_{in}^{d} = (V_m \cdot \sin^2(\omega t)) + (V_m \cdot \cos^2(\omega t)) \tag{11}$$

where V_m is an peak value of normalized voltage, V_{in}^{d} and ω is an instantaneous magnitude of the normalized source voltage and the line frequency respectively.

V_{in}^{d} is the instantaneous magnitude of the normalized source voltage and this can be utilized as detection of voltage sag or swell. When V_{in}^{d} =1, there is no voltage disturbance in the source voltage and no compensation is required. In case of a sag, V_{in}^{d} is less than 1 and in case of a swell, it is greater than 1. A Figure.18 shows the example of 30% voltage sag detection by utilizing algorithm.

In this control scheme, a compensating voltage reference, $V_{c,ref}$ is defined in order to make zero in condition of nominal voltage signal. The compensating voltage reference, $V_{c,ref}$ for voltage sag or swell is determined by subtracting $V_{in,d}$ signal from normalized reference voltage signal $V_{o,ref.}$ These are described as

$$V_{c,ref} = \begin{cases} 0 & (\text{no sag or swell}) \\ > 0 & (\text{sag case}) \\ < 0 & (\text{swell case}) \end{cases} \tag{13}$$

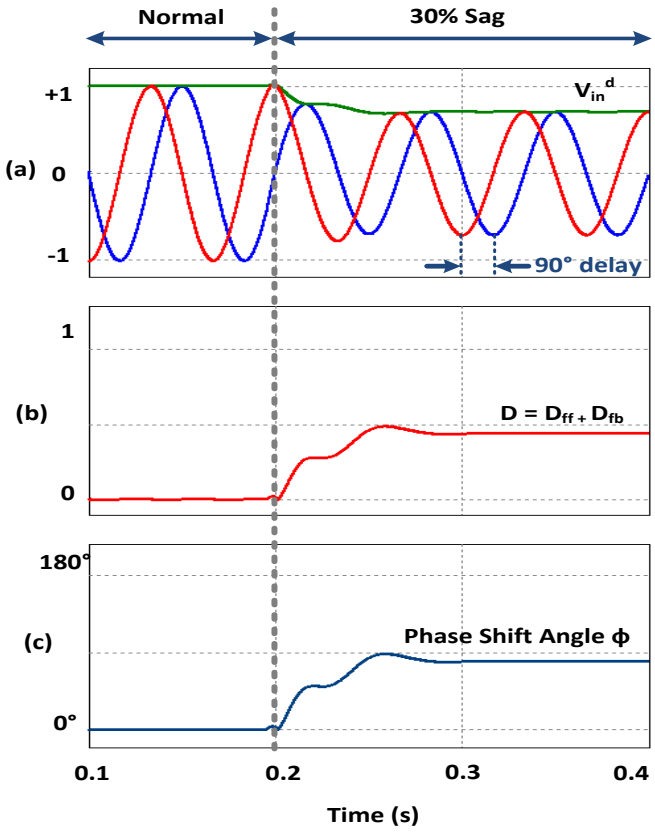

Figure 18. Operation for Voltage Sag Detection (a) V_{in}^{d} (b) Duty Ratio (c) Phase Shift Angle, Φ.

3.4. Generation of Phase Delay Angle, ϕ

After adding a nominally small numerical constant to avoid a zero denominator, the calculated duty ratio D_{ff} from feedforward loop can be expressed as

$$D_{ff} = \frac{\left|1 - V_{in}^{d}\right|}{V_{in}^{d}} = \frac{\left|V_{c,ref}\right|}{V_{in}^{d}} \tag{14}$$

The feedback PI (Proportional-integral) controller is designed to make steady-state error zero. The duty ratio D_{fb} as calculated by the feedback control can be expressed as

$$D_{fb} = k_p \cdot (1 - U_{load}) + k_i \cdot r(t) \tag{15}$$

$$\frac{dr(t)}{dt} = (1 - U_{load}) \tag{16}$$

where U_{load} is the instantaneous value of normalized load voltage and k_P, k_i are proper proportional and integral gains respectively. In addition, *r(t)* represents the integral of the load voltage error ΔU_{load} and this integral part performs to zero-steady state error. The duty ratio can be expressed as shown in (17) and (18).

$$D = D_{ff} + D_{fb} \tag{17}$$

$$D = \left| \frac{1 - U_{grid}}{U_{grid}} \right| + \left[k_p \cdot (1 - U_{load}) + k_i \cdot r(t) \right] \tag{18}$$

The angle of phase delay (ϕ) can be obtained using (18). ϕ is limited within the range of 0° to 180°. ϕ can be obtained by (19).

$$\phi = 180 \cdot \frac{N_s}{N_p} \cdot \left[\left| \frac{1 - U_{grid}}{U_{grid}} \right| + k_p \cdot (1 - U_{load}) + k_i \cdot r(t) \right] \tag{19}$$

where $\phi \in [0, 180]$

When the grid voltage has no disturbance, the phase shift angle will be zero and the compensating voltage will be zero. If a voltage disturbance occurs, the controller varies the phase-shift angle dynamically to compensate for the sag or swell. This phase angle and voltage combination is used to generate the switching functions of the four converters in the smart distribution transformer system.

3.5. Operation for Phase Shift Modulation in the Proposed Control

In this subsection, the operation of the proposed control strategy is described in waveform as shown in Figure.19. Figure.19 (a) represents that 50% sag condition, nominal voltage, and 50% swell condition with per unit. According to equation (11), the direct axis component of the input voltage, V_{in}^{d} is obtained as shown in Figure.19(b). A compensating voltage reference, $V_{c,ref}$, as expressed in equation (13),which is subtracted $V_{in,}^{d}$ signal from normalized reference voltage signal $V_{c,ref}$ is shown in Figure.19(c). Thus, Figure.19 (d) represents the calculated duty ratio D_{ff} from feedforward loop as expressed in (14). The angle of phase delay (ϕ) in the control scheme is obtained by a conversion of the duty ratio to radian after adding D_{ff} and D_{fb} as seen in Figure.19 (e).

As shown in Figure.19 (f), the primary voltage, V_{pri} is generated HF based on the obtained phase shift angle ϕ from the control scheme. Assumed 1:1 MF/HF transformer is selected, the compensating voltage for 50% sag condition can be generated by superimposed the maximum phase angle ϕ which is $\boldsymbol{\pi}$ in rad on the 50% sagged line frequency pulsating voltage as shown in Figure.19(f),(g) and (h). For the 50% swell condition, the primary voltage has $\frac{2\pi}{3}$ in rad phase delay superimposed on a line frequency swelled pulsating voltage as shown in Figure.19(f). The 180° out-of-phase compensating voltage V_c is provided by filtering out HF components from unfolded voltage as shown in Figure.19 (g) and (h).

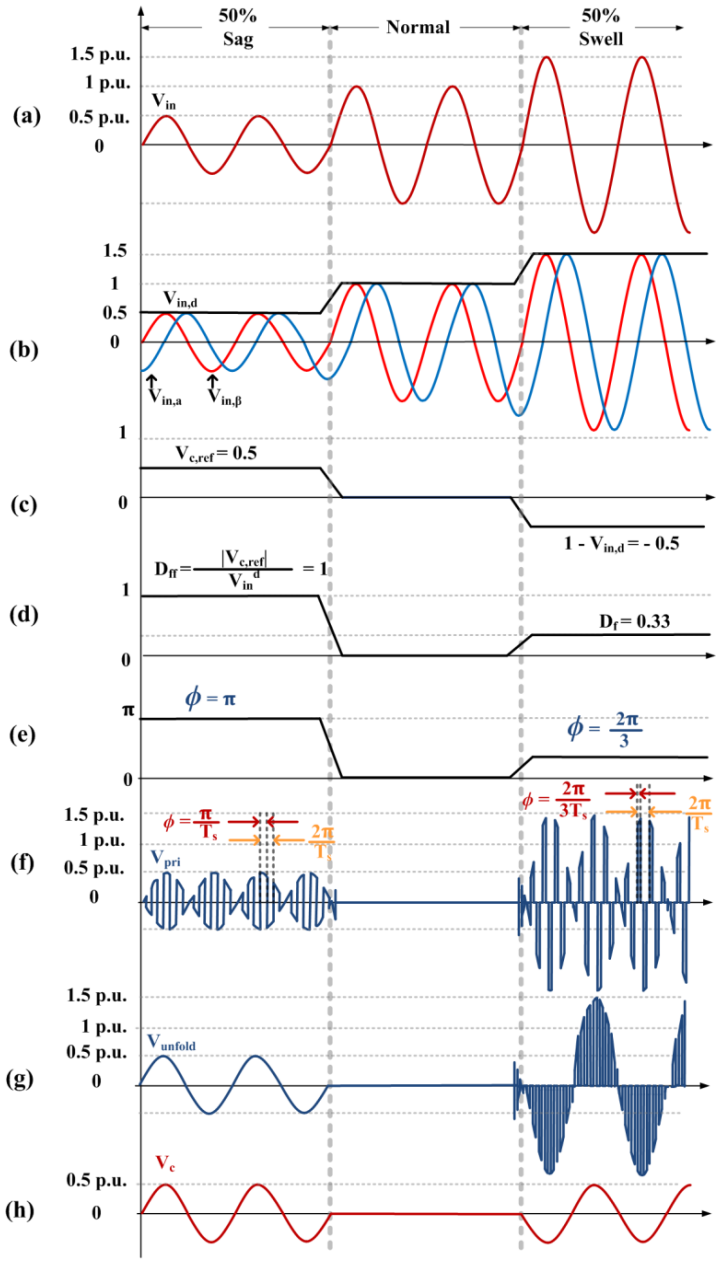

Figure 19. Ideal Operation for Phase Shift Modulation in the Proposed Control Scheme At 1:1 Turns Ratio (a) Source Voltage V_{in} with 50% Sag, Normal and 50% Swell (b) Normalized Source Voltage, 90° Phase Delay Normalized Source Voltage and Normalized Direct Axis Voltage – $V_{in,A}$, $V_{in,B}$ and $V_{in,D}$ (c) Error Signal of Normalized Voltage, $V_{c,Ref}$ (d) Duty, D_{ff} (e) Phase Shift Angle Φ (f) Primary Voltage of MF/HF Transformer, V_{pri} (g) Unfolded Voltage, V_{unfold} (h) Compensating Voltage *Vc*.

3.6. Conclusion

The closed loop control was explained in this chapter. The proposed control system mainly consists of two loops – (a) Load voltage control block with feedback control and (b) Compensating voltage reference generation block with feedforward control. The objective of the control strategy is to derive the phase shift angle, ϕ and this is utilized to determine the amount of compensating voltage as discussed in previous section. The angle of phase delay (ϕ) in the control scheme is obtained by a conversion of the duty ratio to radian after gaining each duty ratio from feedback control loop and feedforward control loop respectively.

4. MATHEMATICAL MODELING AND SIMULATION RESULTS

4.1. Introduction

This chapter presents a modeling and simulation results from engineering software tools in different conditions of voltage sag and swell.

4.2. Mathematical Modeling Results: Principal Operation

In this section, the principal operation waveforms of power electronics module are described. Figures.20 and 21 represents the principal waveform of power electronics module as discussed in previous chapter 2. Matlab 2014 software was utilized in order to obtain mathematical modeling.

The results in Figures.20 and 21 show the waveforms for the input voltage, rectified dc voltage, switching function, the *MF/HF* transformer primary voltage, folded voltage, the unfiltered unfolded voltage and load voltage of the *PE* module, respectively. The rectified dc voltage contains a double frequency ripple, as evidenced by its frequency spectrum as discussed in previous chapter 2. The voltage applied to the primary side of the transformer contains high frequency components. For this reason, it is possible to utilize *MF/HF* transformer in the power electronics module. The *PE* module output voltage contains a line frequency component (60 Hz) with high frequency harmonics and its harmonics that can be attenuated by a small output filter to regulate load voltage.

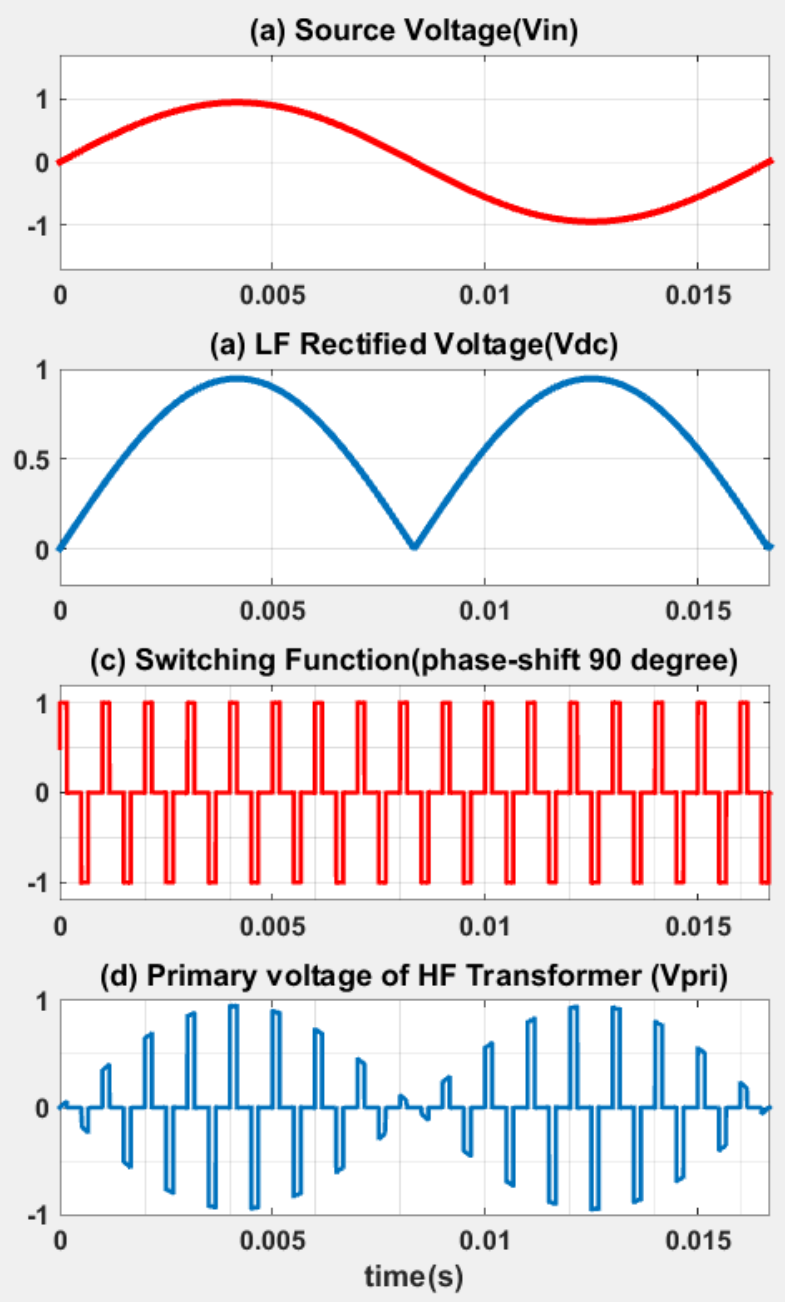

Figure 20. Mathematical Modeling Results (a) Source Voltage, (b) LF Rectified Voltage, (c) Switching Function (d) Primary Voltage of HF Transformer.

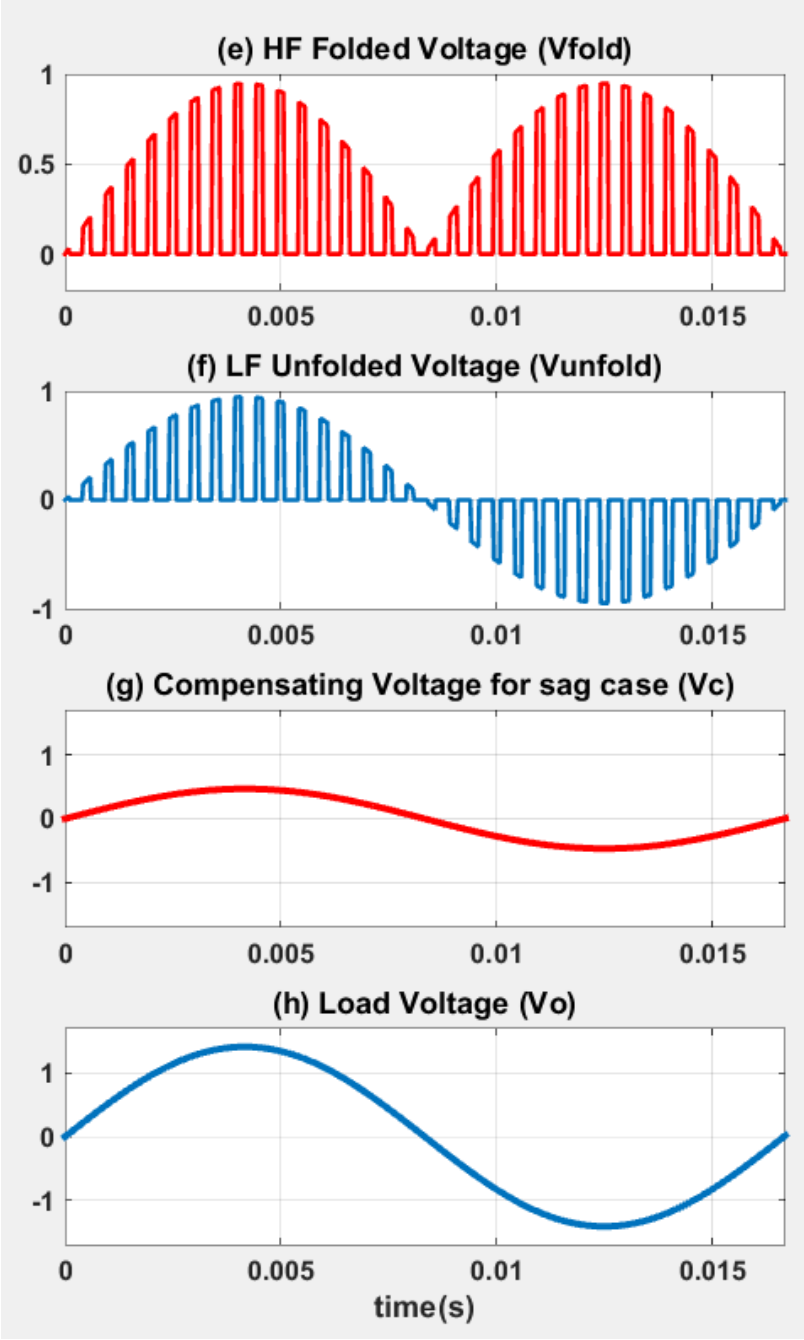

Figure 21. Mathematical Modeling Results (e) HF Folded Voltage, (f) LF Unfolded Voltage, (g) Compensating Voltage (h) Load Voltage.

4.3. Simulation Specification of the Proposed System

The proposed smart distribution transformer was simulated with the closed loop control strategy explained in previous chapters for the conditions in Table 7. The proposed smart distribution transformer was simulated with the proposed control scheme, for a power rating of 15kW at medium voltage grid input. The simulation is employed by PSIM v.9.4 software with following conditions.

TABLE 7: OPERATING CONDITIONS FOR THE PROPOSED SYSTEM DESIGN EXAMPLE

Input voltage	120 V (rms) 60 Hz
Switching Frequency	10kHz
Input filter components	L_i = 1 mH , C_i = 15 µF
Load power	15 kW
MF/HF transformer Turns Ratio	N_p:N_s = 1: 1
Output filter components	L_o = 4 mH, C_o = 7.5µF

4.4. Dynamic Capability for Operating Mode and Bypass Mode

Figure.22 shows the dynamic operating mode and bypass mode in the PE module with their corresponding frequency spectra (FFT). The transformer high frequency was selected to be 10kHz with 1:1 turns ratio. It is observed that there is less than half-cycle detection time between a normal and a sag event. This is attributed to the half-cycle delay time in the voltage peak detection algorithm to calculate the phasor of the voltages. In Figure.22 (j), the primary voltage frequency spectrum shows the HF (10k ± 120)Hz

components while line frequency (60Hz) is observed in source and load voltage as shown in Figure.22 ((h), (i) and (j)).

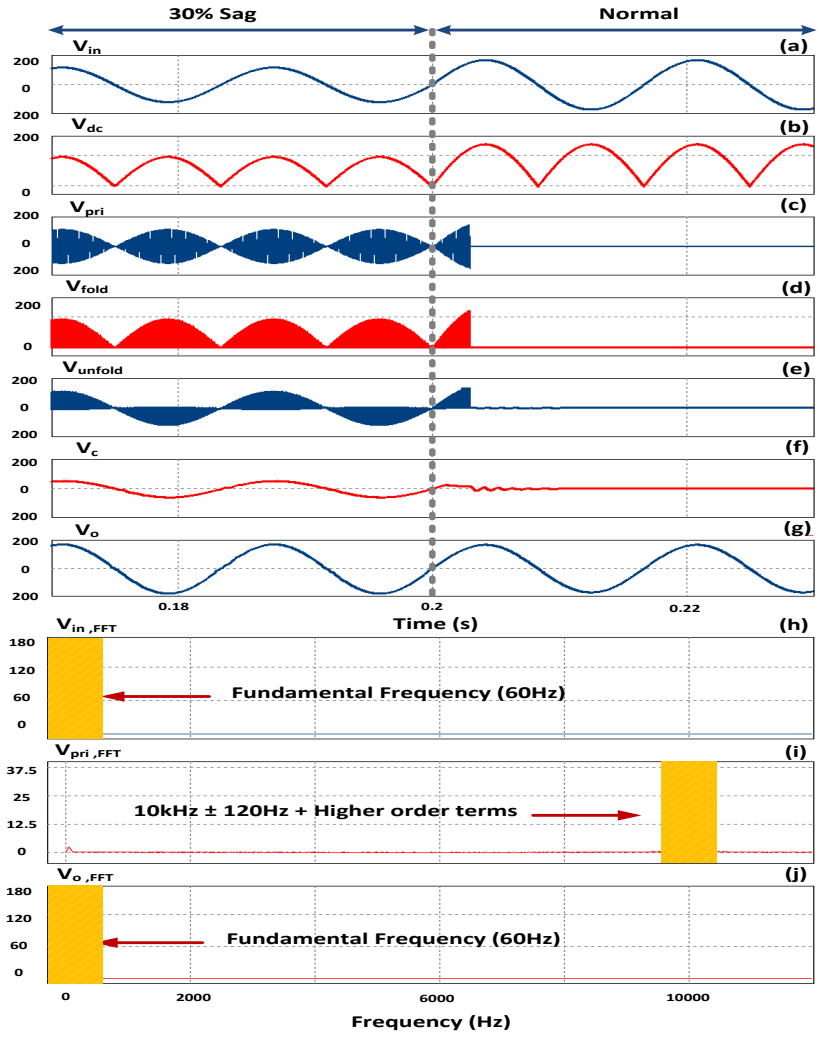

Figure 22. Operating Mode Simulation Results of the PE Module for the 30% Sag Case (a) Source Voltage, V_{in} (b) Rectified Voltage, V_{dc} (c) Primary Voltage, V_{pri} (d) Folded Voltage, V_{fold} (e) Unfolded Voltage, V_{unfold} (f) Compensating Voltage, V_c (g) Load Voltage, V_o (h) Frequency Spectrum for Source Voltage, V_{in} (i) Frequency Spectrum for Primary Voltage, V_{pri} and (j) Frequency Spectrum for Load Voltage, V_o.

4.5. Voltage Sag Compensation

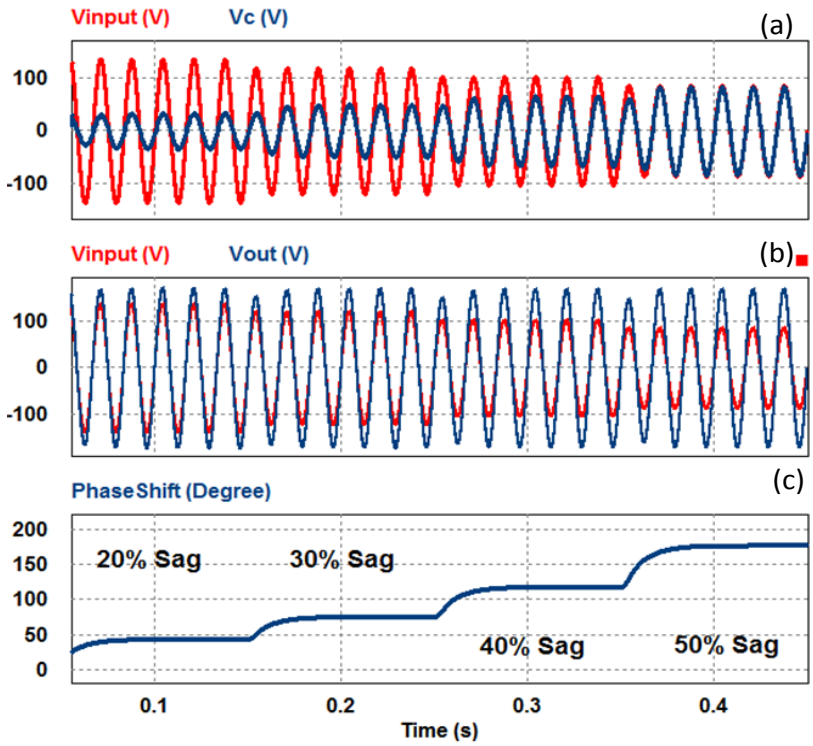

Figure 23 Dynamic Compensating Responses for Sag Condition from 20% to 50% (a) Source Voltage and Compensating Voltage (b) Source Voltage and Load Voltage (c) Phase-Shift Angle.

The occurrence of a 20% to 40% single-phase sag condition are studied as seen in Figure.23. During the first 0.1 s, there is a 20% sag followed by different sagged voltage inputs during subsequent 0.1 s intervals as seen in Figure.23(c) with increasing phase shift angle. Since the *MF/HF* transformer turns ratio is 1:1, the phase shift angle is 180° in degree for the 50% sag condition. Also it is noted that the compensating voltage from

PE module (V_c) was in-phase with the input voltage, so that the two voltages added up in magnitude in Figure.23(a).

4.6. Voltage Swell Compensation

On the other hand, during swell conditions (Figure.24) the compensating voltage is 180° from the grid side voltage, leading to a subtraction and the output voltage is now regulated to the desired reference value as seen in Figure.24 (a). Additionally, the corresponding phase-shift angle varies dynamically based on the input voltage, as seen in Figure.24 (c). It is also observed that the phase-shift angle during the sag case is greater (Figure.23) than that of the swell case (Figure.24) for same percentage value of sag and swell.

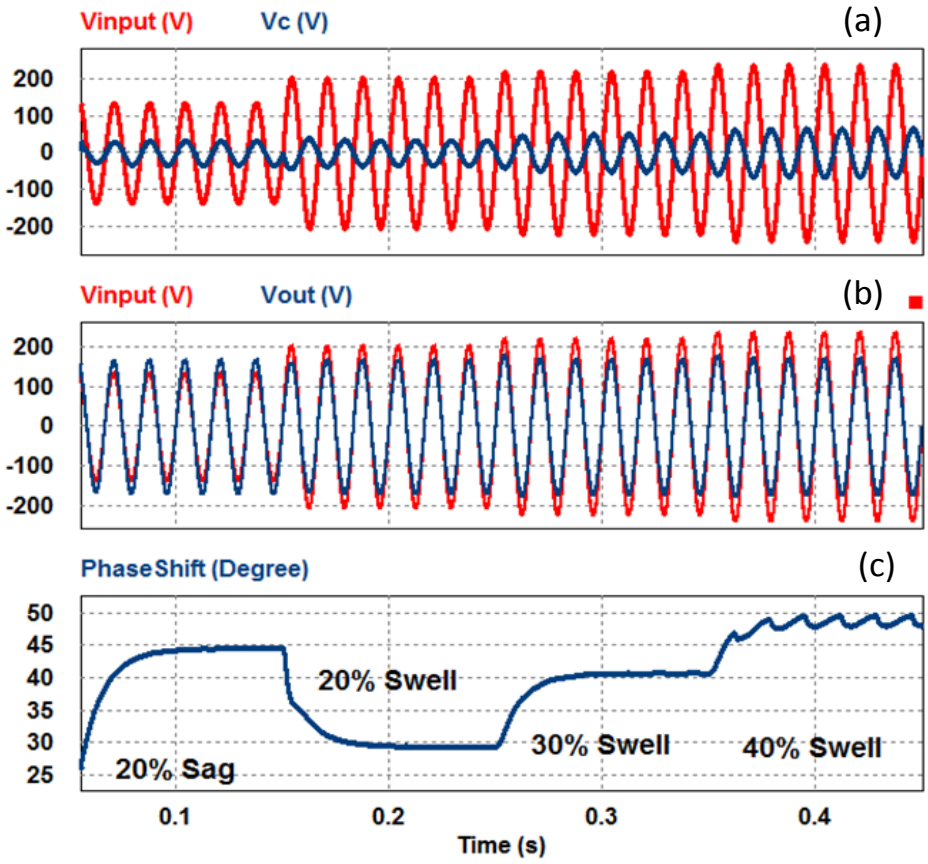

Figure 24. Dynamic Compensating Responses for Sag (20%) and Swell Condition from 20% to 40% (a) Source Voltage and Compensating Voltage (b) Source Voltage and Load Voltage (c) Phase-Shift Angle.

4.7. Dynamic Performances for Voltage Sag and Swell

Figure.25 shows the input voltage, compensating voltage, and load voltage when the input voltage has a 40% sag and 40% swell. The phase of the compensating voltage for sag is a 180° phase delay from that of swell condition and a load voltage, V_o is compensated by adding source voltage V_{in} to compensating voltage V_c. Also it is observed that the output voltage is kept constant at 120V for input voltages disturbance as shown in Figure.25 (c).

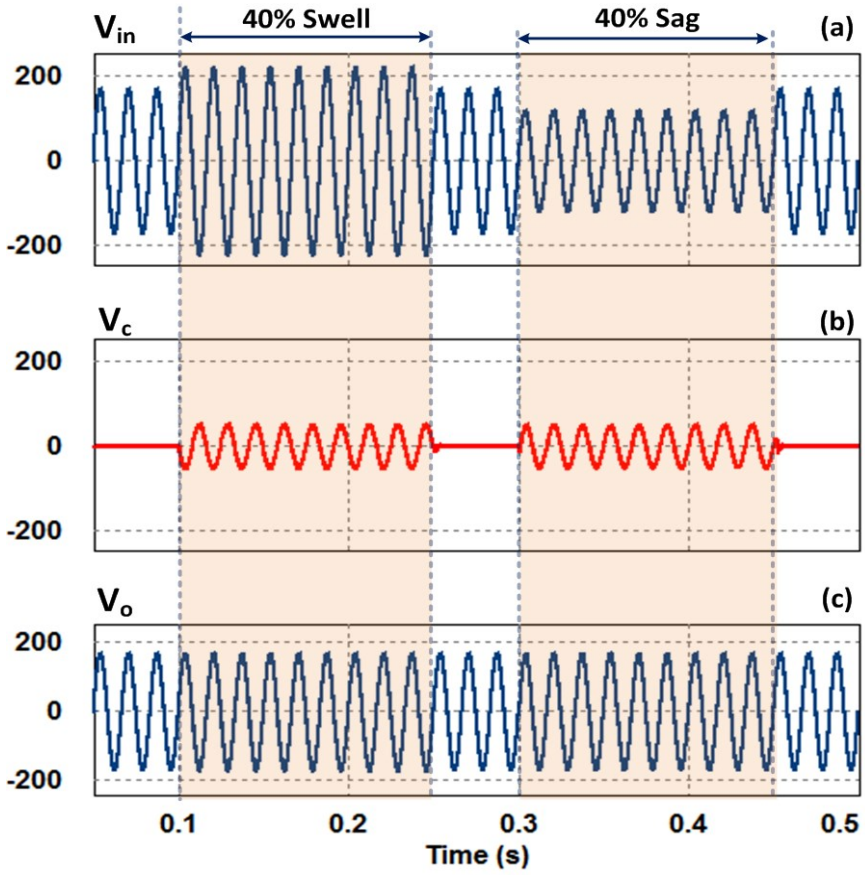

Figure 25. Dynamic Compensating Responses for Sag (40%) and Swell Condition (40%) (a) Source Voltage, V_{in} (b) Compensating Voltage, V_c and (c) Load Voltage, V_o.

The dynamic performance of the phase shift angle variation with a linear load is shown in Figure.26. The occurrence of a 50% sag to 50% swell is emulated in the input. The phase shift angle is reduced in every 10% diferent sag condition and become zero during the normal condition. During the swell condition, the variation of the phase shift angle is relatively less steep compared to that of sag condition as seen in Figure.26.

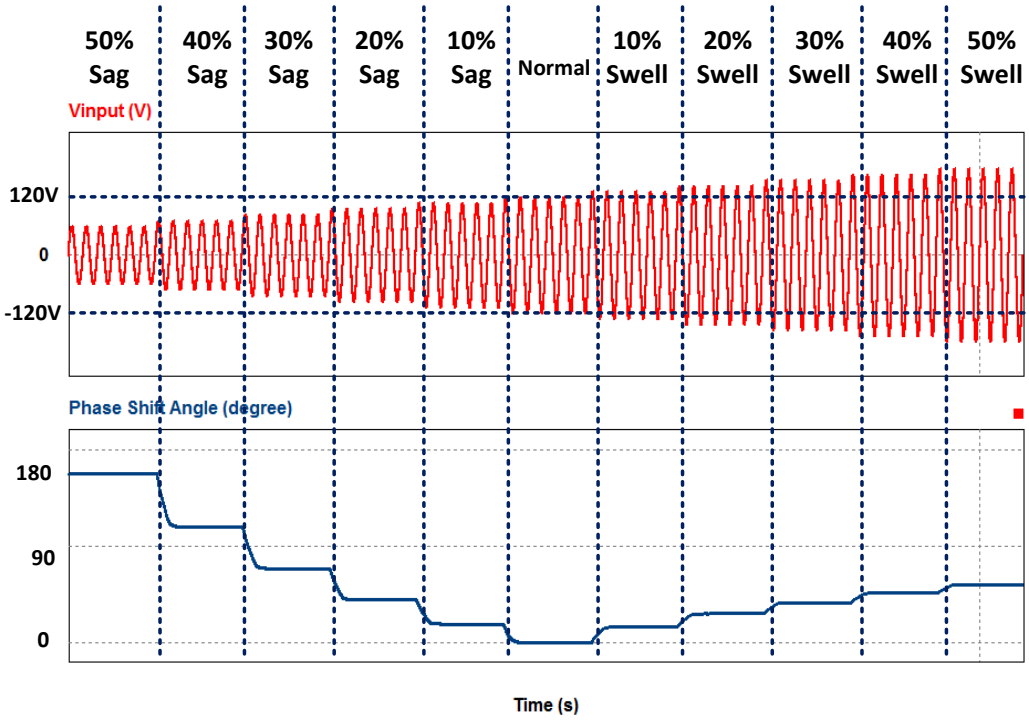

Figure 26. Dynamic Performance for Phase Shift Angle Variation in Different Sag and Swell Conditions.

4.8. Conclusion

Overall system simulation results of 15kW were shown in different voltage disturbance conditions and the variation of phase shift angles is also presented in terms of amount of voltage disturbance by utilizing software tools.

5. EXPERIMENTAL SETUP AND RESULTS

5.1. Introduction: Laboratory Setup and Experimental Conditions

The experimental results obtained for power electronics module with voltage disturbance are discussed in this chapter. A scaled-down 1.5kW laboratory prototype for the proposed system was constructed and tested as shown in Figures.27 and 28. The operating condition, devices rating and MF/HF transformer design parameters are shown in Tables 7, 8 and 9. The controller was implemented with the Texas Instruments TMS320F28335 controller and the power devices used were Semikron IGBT modules.

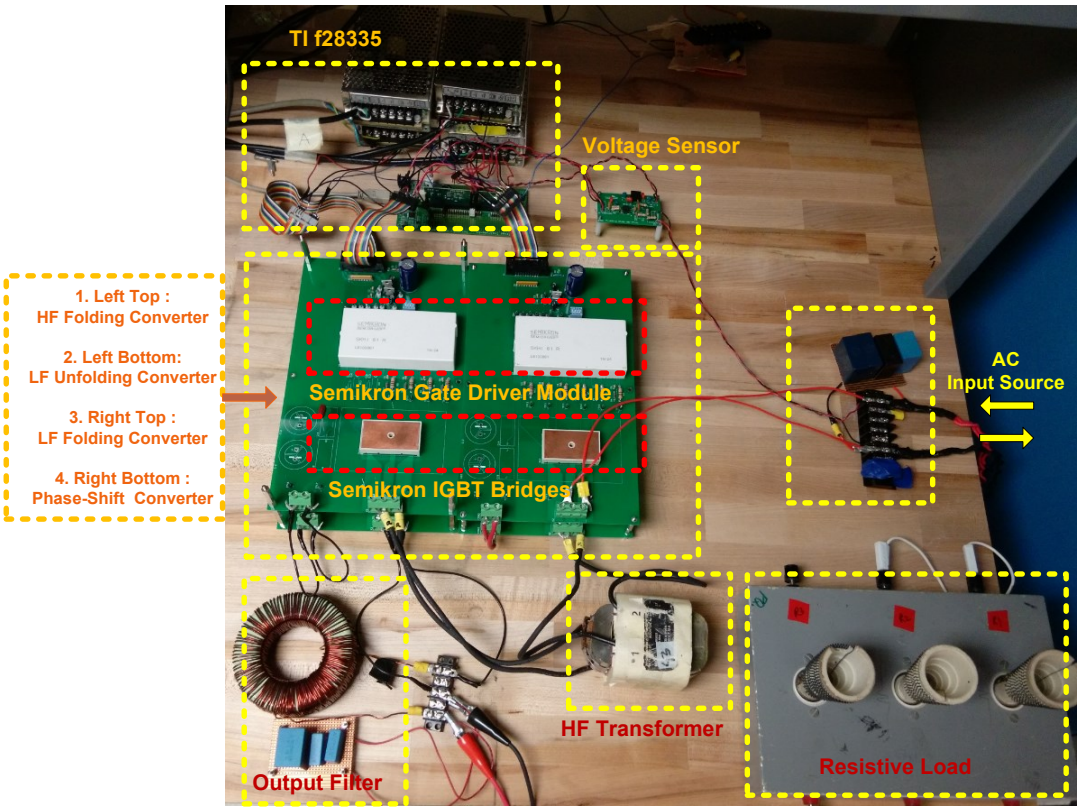

Figure 27. Laboratory Experiment Setup (Without Package Box).

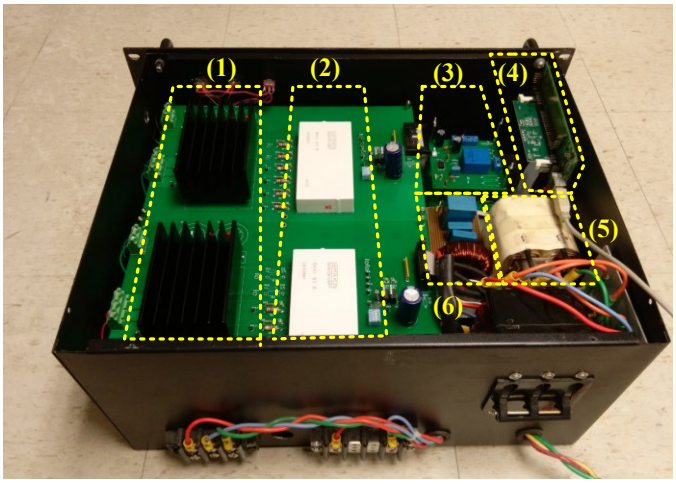

(1) IGBT modules **(2) Gate Drivers**
(3) Voltage Sensors **(4) DSP controller**
(5) HF Transformer **(6) Output Filter**

Figure 28. Prototype of the Power Electronics Module (With Package Box).

TABLE 8: OPERATING CONDITIONS FOR THE PROPOSED SYSTEM

Input voltage	120 V_{rms} / 60 Hz
Load power	1.5 kW
Max Sag Compensation Capability	50%
Max Swell Compensation Capability	50%

TABLE 9: COMPONENT RATINGS OF THE PE MODULE

DEVICES	RATING
IGBT Devices (S_1-S to Q_1-Q_4 of HF converters and switches of LF converters)	250V (1.5 p.u.) 6 A_{rms} (0.5 p.u.)
Output Filter Inductor L_f = (4 mH)	12 A_{rms} (1 p.u.)
Output Filter Capacitor C_f = (7.5μF)	85V (0.5 p.u.)
Small coupling capacitor C_{dc} = (0.8μF)	250 V (1.5 p.u.)

TABLE 10: SUMMARY OF PARAMETER FOR HF TRANSFORMER

Phase Type	Single Phase
Core Material	Si-Steel
Operating Switching Frequency, f_s (Hz)	3000
Turns Ratio	1:1
Peak Flux Density, B_{peak} (Tesla)	2.0
Input / Output Voltage RMS (V)	80/80
Rated VA	850
Number of Turns in Primary Side (# of strands)	7 (3)
Number of Turns in Secondary Side (# of strands)	7 (3)

5.2. Experiment Results

The device ratings are determined based on the change in voltage during swell condition. In other words, the compensation capability for swell voltage depends on the device rating while the compensation for sag case is determined by HF transformer turns ratio. In this experiment, two IGBTs S_{3_M4} and S_{4_M4} in the unfolding converter (M_4) were utilized as bypass switches in Figure.10 turning on at the same time during bypass mode.

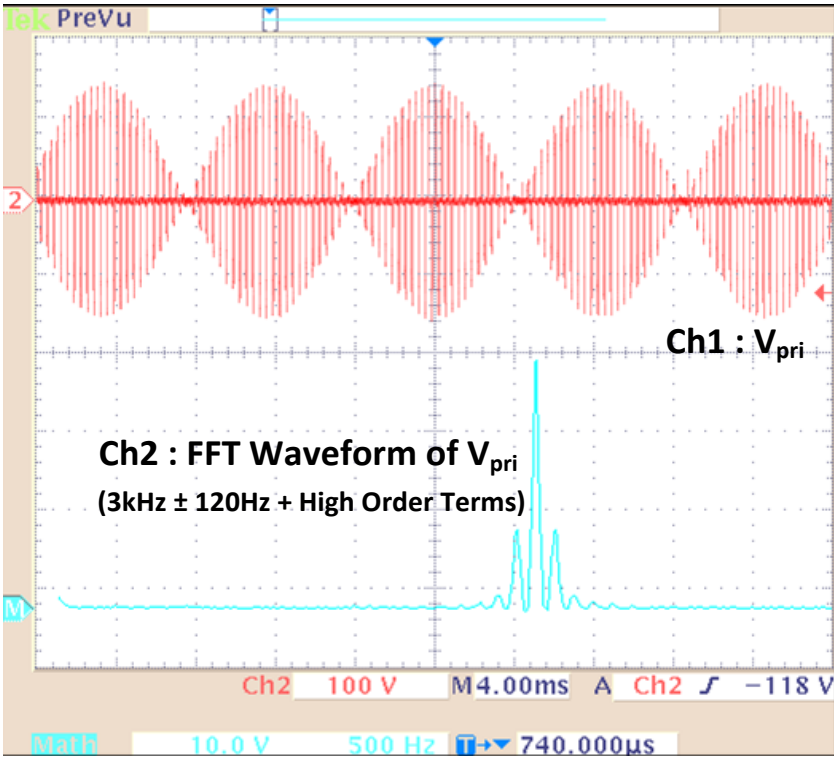

Figure 29. Ch1 : Primary Voltage of Transformer V_{pri} and Ch2 : Frequency Spectrum.

Figure.29 shows the primary voltage of the HF transformer. The HF quasi-pulsating dc voltage V_{pri} can be seen in Ch1 and the frequency spectrum of Ch2 shows a 3 kHz switching frequency along with ±120 Hz components as derived in (3).

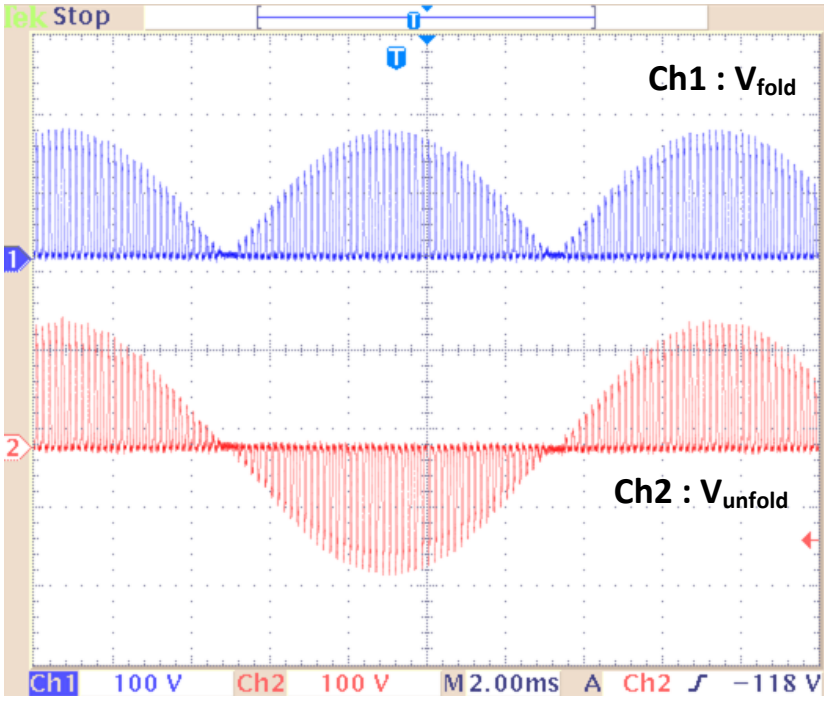

Figure 30. Ch1 : Folded Voltage, V_{fold} and Ch2 : Unfolded Voltage, V_{unfold}.

In Figure.30, folded voltage including HF components (V_{fold}) can be seen in Ch1. By 60 Hz unfolding switching operation, the HF fixed duty chopped 60 Hz sinusoidal voltage (V_{unfold}) is obtained, shown in Ch2. This unfolded voltage becomes the compensator output voltage V_c after HF components are filtered out, to generate the nominal voltage 120V.

The dynamic compensating operation of the proposed system is shown in Figures 31, 32 and 33 in various conditions. Figures. 31, 32 and 33 shows that the load voltage V_o is well regulated with a nominal 120V by the proposed system. The corresponding voltage waveforms when the input voltage has 50% and 40% sags are shown in Figure. 31. Figure. 32 shows that consequent 18 cycles of 25% and 37% voltage swell conditions respectively are compensated in the 120V nominal load voltage.

Figure 33 shows a dynamic response of compensation for both of sag and swell conditions. It is also observed that the load voltage is compensated to the desired 120V within a half cycle. There exists a voltage overshoot at the instant of voltage recovery caused by the detection delay in the control algorithm.

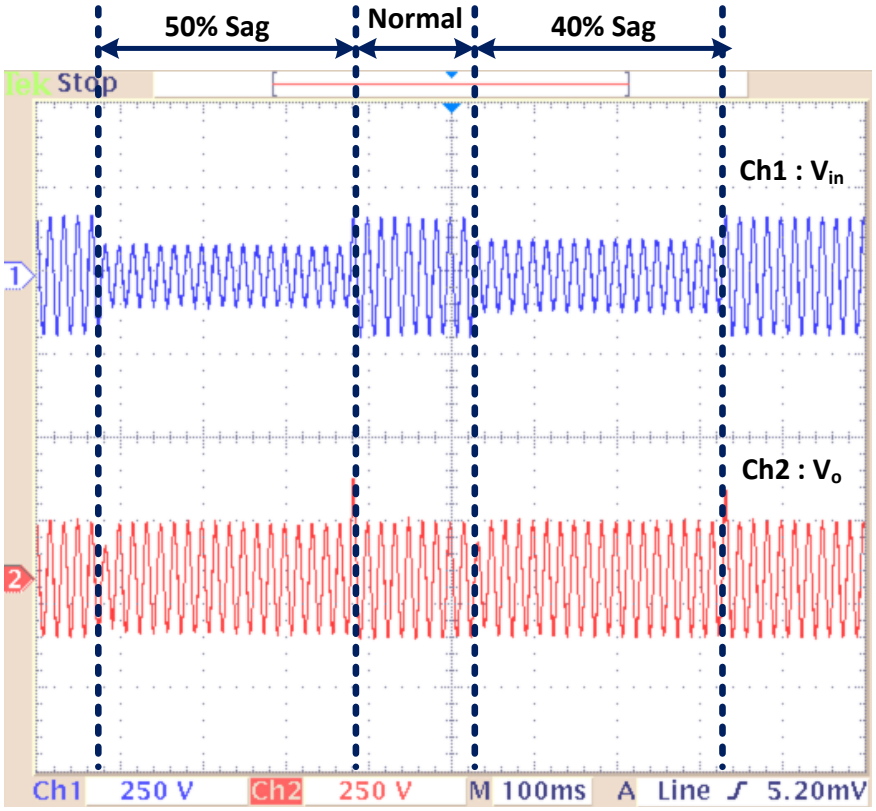

Figure 31. Ch1 : Source Voltage with 50% Sag and 40% Sag Respectively Ch2 : Compensated Load Voltage.

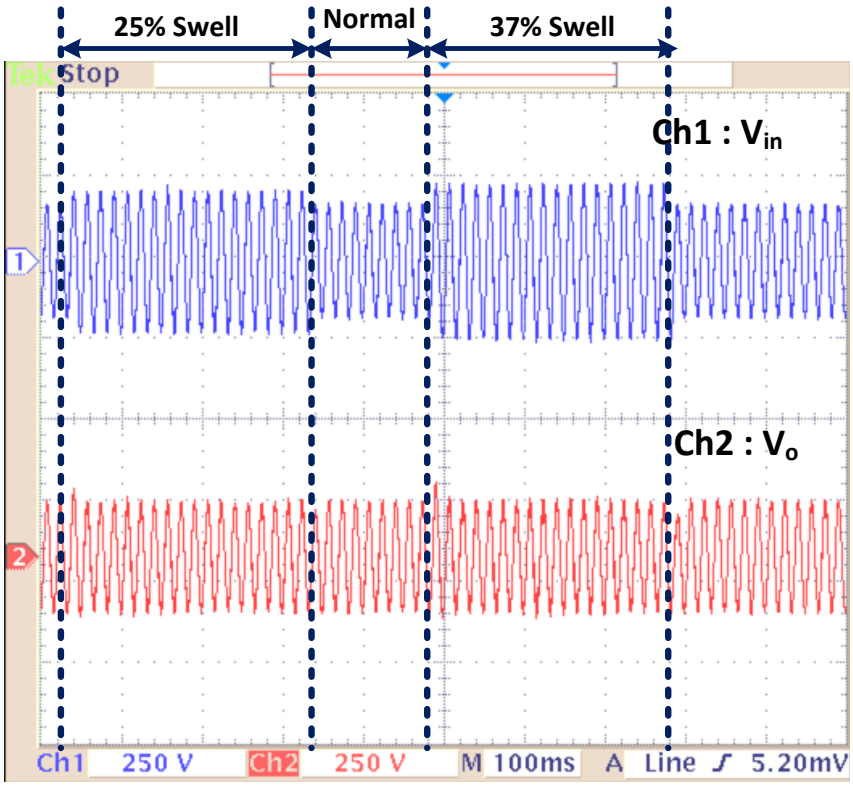

Figure 32. Ch1 : Source Voltage with 25% Swell and 37% Swell Respectively Ch2 : Compensated Load Voltage.

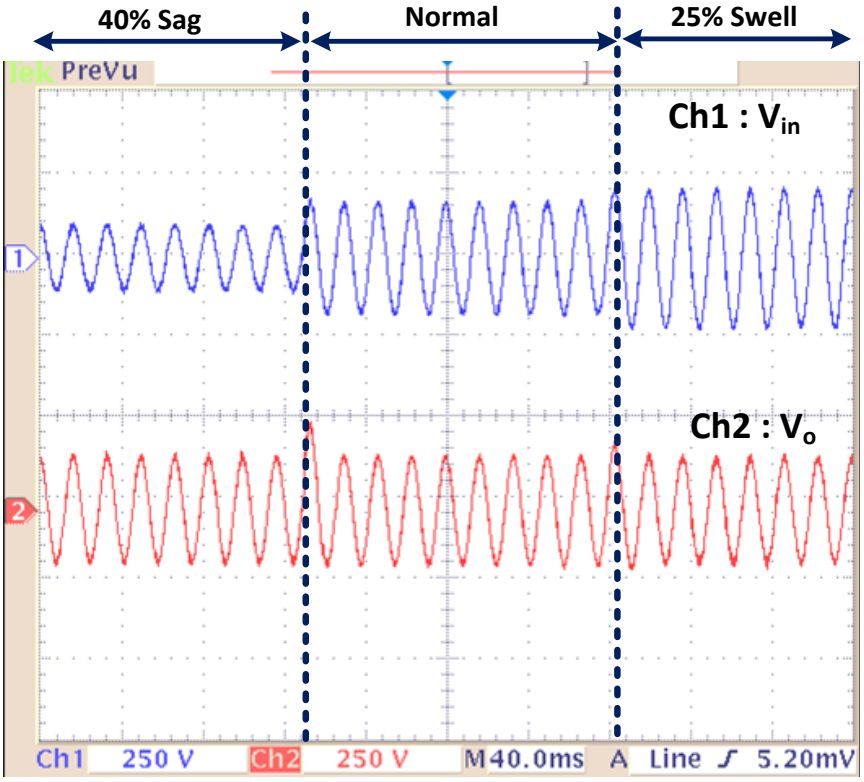

Figure 33. Ch1 : Source Voltage with 40% Sag and 25% Swell Respectively Ch2 : Compensated Load Voltage.

5.3. Conclusion

The laboratory scaled down prototype of the proposed system was presented. This experimental result showed the dynamic voltage compensation in various sag or swell condition. Based on the results, the proposed system with 1:1 turns ratio of 3kHz HF transformer in this hardware set-up is verified to regulate load voltage in order to improve power quality. By utilizing higher frequency transformer, the overall size and weight of the power electronics module can be reduced. Moreover, a selection of devices and components can be determined by the application of the load or the required an amount of compensating voltage to the load side.

6. SUMMARY

6.1. Conclusion

In this thesis, a smart distribution transformer for the smart grid was proposed. The proposed approach can be integrated into a conventional distribution transformer to add sag or swell compensation functionality. Results obtained demonstrate compensation for voltage sag/swell and the proposed system is capable of mitigating steady state voltage distortion. Also, the PE module has a lower voltage rating and the MF/HF transformer has a lower VA rating than the load, due to partial power processing. The proposed system is a possible retro-fit solution to improve power quality in existing distribution transformers for the smart gird**,** especially in the face of the proliferation of renewable and distributed generation**.**

REFERENCES

[1] “Distribution Transformer”, Wikipedia, November 2015. [Online]. Available: https://en.wikipedia.org/wiki/Distribution_transformer

[2] S. Bhattacharyya, J. M. A. Myrzik, and W. L. Kling, “Consequences of poor power quality: An overview,” in Proc. 42nd Int. Univ. Power Eng. Conf., pp. 651–656, 2007.

[3] Mohibullah, Laskar, S.H. “Power Quality Issues and Need of Intelligent PQ Monitoring in the Smart Grid Environment,” 47th Universities Power Eng. Conf., (UPEC), pp 1-6, 2012.

[4] J. Kyei, R. Ayyanar, G. T. Heydt, R. Thallam, J. Blevins, “The design of power acceptability curves,” IEEE Trans Power Deliv., vol.17 pp. 828–833, 2002.

[5] Brumsickle, W.E.; Schneider, R.S.; Luckjiff, G.A.; Divan, D.M.; Mc Granaghan, M.F.; “Dynamic sag correctors: cost-effective industrial power line conditioning”, IEEE Transactions on Industry Applications, vol: 37, No. 1, pp: 212 –217, 2001.

[6] O. C. Montero Hernandez, P. Enjeti, “A Low Cost Approach to Provide Ride-Through for Critical Loads”, 16th Annual IEEE Applied Power Electronics Conference and Exposition, vo1. 2, pp. 917-923, 2001.

[7] Aeloiza, E.C.; Enjeti, P.N.; Montero, O.C.; Moran, L.A. "Analysis and design of a new voltage sag compensator for critical loads in electrical power distribution systems", Conference Record of the 37th IAS Annual Meeting., pp: 911 - 916 vol.2 Volume: 2, 13-18 Oct. 2002.

[8] M.S. Calovic, “Modeling and analysis of under-load tap changing transformer control systems”, IEEE Transactions on Power Apparatus and Systems, Vol. 103, pp. 1909-1915, 1984.

[9] N. Yorino, M. Danyoshi and M. Kitagawa, “Interaction Among Multiple Controls in Tap Change Under Load Transformers”, IEEE Transactions on Power System, vol. 12, no. 1, pp. 430434, Feb. 1997.

[10] Q. Wu, D. H. Popovi´c, and D. J. Hill, “Avoiding sustained oscillations in power systems with tap changing transformers,” *Int. J. Elect. Power Energy Syst.*, vol. 22, no. 8, pp. 597–605, Nov. 2000.

[11] I. G. Nielsen, M. Newman, H. Nielsen and F. Blaabjerg. “Control and testing of a dynamic voltage restorer DVR) at medium voltage level”, IEEE Trans. Power Electronics, vol. 19, pp. 806-813. May 2004.

[12] A. K. Sadigh and K. M. Smedley, “Review of voltage compensation methods in dynamic voltage restorer (DVR),” in Proc. IEEE Power Energy Soc. Gen. Meet., Jul. pp. 1–8, 2012.

[13] S. S. Choi, J. D. Li, and D. M. Vilathgamuwa, “A generalized voltage compensation strategy for mitigating the impacts of voltage sags/swells,” IEEE Trans. Power Delivery, vol. 20, no. 4, pp. 2289–2297, Jul. 2005.

[14] S. Lee., H. Cha, B. Han, “A new single-phase voltage sag/swell compensator using direct power conversion”, in Proc. Energy Conversion Congress and Exposition, 2009. pp 2704-2710, 2009.

[15] S. Bala, D. Das, E. Aeloiza, A. Maitra, and S. Rajagopalan, “Hybrid distribution transformer: Concept development and field demonstration,” in Proc. IEEE Energy Convers. Congr. Expo, pp. 4061–4068, 2012.

[16] Sastry, J., Bala, S. "Considerations for the design of power electronic modules for hybrid distribution transformers", Energy Conversion Congress and Exposition (ECCE), IEEE,On page(s): 1422 – 1428, 2013.

[17] Radi, M.A., Darwish, M.; Alqarni, M. "Voltage regulation considerations for the design of hybrid distribution transformers", Power Engineering Conference (UPEC), 2014 49th International Universities, On page(s): 1 – 6, 2014.

[18] “The Feasibility of replacing or upgrading utility distribution transformers during routine maintenance”, Power Systems, Tech prog Oak Ridge National Lab, Tennessee, USA, Final Rep. DOE AC05840R2140000, April, 1995

[19] X. She, A. Huang, and R. Burgos, “Review of solid-state transformer technologies and their application in power distribution systems,” IEEE J. Emerging Sel. Topics Power Electron., vol. 1, no. 3, pp. 186–198, Sep.2013.

[20] Hafez, B. Krishnamoorthy, H.S. ; Enjeti, P. ; Ahmed, S. ; Pitel, I.J.“ Medium voltage power distribution architecture with medium frequency isolation transformer for data centers”, Applied Power Electronics Conference(APEC), IEEE, On pp. 3485-3489, 2014.

[21] Krishnamoorthy, H. S.; Rana, D.; Enjeti, P. N.; “A new wind turbine generator / battery energy storage utility interface converter topology with medium-frequency

transformer", Applied Power Electronics Conference & Exposition (APEC) 2013, Long Beach, CA

[22] Kang, T.; Essakiappan, S.; Enjeti, P.; Choi, S.; "Towards a smart distribution transformer for smart grid", 9th International Conference on Power Electronics and ECCE Asia(ICPE-ECCE Asia) 2015, Seoul, South Korea, pp. 1997-2003.